

**FIELD EQUILIBRIUM FINITE ELEMENTS
FOR STRUCTURAL ANALYSIS**

A THESIS

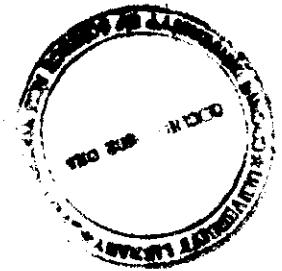
Submitted by

S. JAYAKUMAR

for the award of the degree

of

DOCTOR OF PHILOSOPHY



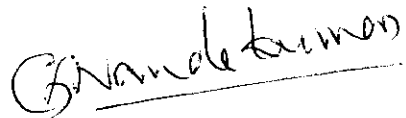
**DEPARTMENT OF SHIP TECHNOLOGY
COCHIN UNIVERSITY OF SCIENCE AND TECHNOLOGY
KOCHI - 682 022**

MARCH 2003

Certificate

*I here by certify that to the best of my knowledge, the thesis entitled **Field Equilibrium Finite Elements for Structural Analysis** is a record of bona fide research carried out by Sri. Jayakumar. S, Part time research student, Reg. No. 2113 under my supervision and guidance, as the partial fulfilment of the requirement for the award of the Ph.D degree in the faculty of technology. The results presented in this thesis or parts of it have not been presented for the award of any other degree.*

Kochi – 22
21 - 03 - 2003

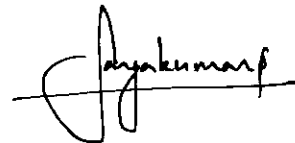


Dr. C.G. Nandakumar
Research Guide
Dept. of Ship Technology
Cochin University of Science and
Technology
Kochi -22

**DECLARATION ABOUT THE AUTHENTICITY OF THE RESEARCH
WORK BY THE RESEARCH STUDENT**

*I here by declare that the thesis entitled **Field Equilibrium Finite Elements for Structural Analysis** is an authentic record of research work carried by me under the supervision and guidance of Dr. C.G. Nandakumar, Department of Ship Technology, in the partial fulfilment of the requirement for the award of the Ph.D degree in the faculty of technology and no part thereof has been presented for the award of any other degree.*

Kochi -22
21-3-2003



Jayakumar. S
Part time Research Student
Reg. No. 2113
Dept. of Ship Technology
CUSAT
Kochi -22

CONTENTS

	Page
ACKNOWLEDGEMENTS.....	i
ABSTRACT	ii
LIST OF TABLES	iii
LIST OF FIGURES	iv
NOTATIONS.....	vi
1. INTRODUCTION	
1.1 Motivation.....	1
1.2 Layout	3
2. LITERATURE REVIEW	
2.1 General.....	5
2.2 Development of conforming finite elements	6
2.2.1 Two dimensional and three dimensional finite elements.....	7
2.2.2 Plate elements.	9
2.3 Development of nonconforming finite elements	11
2.3.1 Two dimensional and three dimensional elements.....	11
2.3.1.1 Reduced or selective integration.....	11
2.3.1.2 Addition of bubble modes.....	12
2.3.1.3 Using unequal order of interpolation	13
2.3.1.4 Assumed strain method.....	13
2.3.1.5 Residual energy balancing	14
2.3.1.6 Other general methods	14
2.3.2 Plate elements	15
2.4 Test problems for element performance comparison.....	16
2.5 Scope of the present work.....	16

3.	DEVELOPMENT OF FIELD EQUILIBRIUM FINITE ELEMENTS	
3.1	General.....	18
3.2	Generation of plane stress element	18
3.2.1	Displacement functions	18
3.2.2	Element geometry	19
3.3	Generation of three dimensional element.....	20
3.3.1	Displacement functions	20
3.3.2	Element geometry	22
3.4	Generation of plate bending element.....	23
3.4.1	Displacement functions	23
3.4.2	Element geometry	25
3.5	Generation of stiffness matrices and evaluation of nodal displacements	25
3.6	Software development for the implementation of field equilibrium finite elements	26
3.6.1	General	26
3.6.2	Plane stress elements.....	26
3.6.3	Three dimensional elements	28
3.6.4	Plate bending elements	30
3.7	Numerical investigations on performance of the elements.....	32
4.	PERFORMANCE COMPARISON OF PLANE STRESS ELEMENT (SFCNQ)	
4.1	General.....	33
4.2	Eigenvalue test.....	33
4.3	Problems with in-plane bending	35
4.3.1	MacNeal - Harder thin cantilever beam.....	35
4.3.2	Deep cantilever beam with rectangular elements	37
4.3.3	Distortion test.....	39
4.4	Stress concentration problems	41
4.4.1	Infinite plate with circular cutout at the centre	41

4.4.2	Circular disc with concentrated edge load	42
4.5	Patch tests	43
4.5.1	Constant strain patch test	44
4.5.2	Weak patch test	45
4.6	Remarks	46
5.	PERFORMANCE COMPARISON OF THREE DIMENSIONAL ELEMENT (SFCSS)	
5.1	General	47
5.2	Eigenvalue test	48
5.3	Aspect ratio sensitivity test	49
5.4	Beam tests	50
5.4.1	Slender beam	50
5.4.2	Deep beam	53
5.5	Patch tests	56
5.5.1	Constant strain patch test	56
5.5.2	Weak patch test	57
5.6	Boussinesq Problem	59
5.7	Curved shell test	60
5.8	Remarks	62
6.	PERFORMANCE COMPARISON OF PLATE BENDING ELEMENT (SFCFP)	
6.1	General	63
6.2	Eigenvalue test	63
6.3	Single element test	65
6.4	Convergence test	66
6.5	Remarks	71

7.	CONCLUSION	
7.1	Summary.....	72
7.2	Scope for the future work	73
	REFERENCES	75
	APPENDIX I.....	81
	APPENDIX II	82
	PUBLICATIONS BASED ON THE RESEARCH WORK	83

ACKNOWLEDGEMENTS

I would like to express my deep sense of gratitude to my guide and mentor Dr. C.G. Nandakumar without whom this work would not have been materialised. The pleasure of learning from him during this endeavour will definitely remain etched forever in my memory. No tribute in words or action can match the debt I owe in this regard.

I would like to thank Dr. Dileep K. Krishnan, Head of the Department of ship technology, for having provided the support – both in his official and personal capacities – for this work.

It is my pleasure to place on record my sincere thanks for all guidance and help rendered during the course of this research work, by Prof. E.M.S. Nair, the former Head of the department of ship technology. I owe much to the valuable insight given by Dr. K.P. Narayanan, in the area of finite element analysis.

Words are not enough to describe my thanks to all the faculty members and office staff of Ship Technology Department. Special mention should be made of Sri. Rajesh, Smt. Seenath and Smt. Ajitha for their kind support.

I am very grateful to Dr. Ashalatha Thampuran and Prof. Mahadevan, the former and present Principals of Rajiv Gandhi Institute of Technology, Kottayam for the encouragement provided by them.

I would like to acknowledge many of my friends and colleagues who in various capacities have rendered their help. Very special thanks to Prof. K.T.Subramanyam, Dr. M.S.Jayamohan and Prof. Bino I. Koshy for their kind cooperation.

ABSTRACT

Many finite elements used in structural analysis possess deficiencies like shear locking, incompressibility locking, poor stress predictions within the element domain, violent stress oscillation, poor convergence etc. An approach that can probably overcome many of these problems would be to consider elements in which the assumed displacement functions satisfy the equations of stress field equilibrium. In this method, the finite element will not only have nodal equilibrium of forces, but also have inner stress field equilibrium. The displacement interpolation functions inside each individual element are truncated polynomial solutions of differential equations. Such elements are likely to give better solutions than the existing elements.

In this thesis, a new family of finite elements in which the assumed displacement function satisfies the differential equations of stress field equilibrium is proposed. A general procedure for constructing the displacement functions and use of these functions in the generation of elemental stiffness matrices has been developed. The approach to develop field equilibrium elements is quite general and various elements to analyse different types of structures can be formulated from corresponding stress field equilibrium equations. Using this procedure, a nine node quadrilateral element SFCNQ for plane stress analysis, a sixteen node solid element SFCSS for three dimensional stress analysis and a four node quadrilateral element SFCFP for plate bending problems have been formulated.

For implementing these elements, computer programs based on modular concepts have been developed. Numerical investigations on the performance of these elements have been carried out through standard test problems for validation purpose. Comparisons involving theoretical closed form solutions as well as results obtained with existing finite elements have also been made. It is found that the new elements perform well in all the situations considered. Solutions in all the cases converge correctly to the exact values. In many cases, convergence is faster when compared with other existing finite elements. The behaviour of field consistent elements would definitely generate a great deal of interest amongst the users of the finite elements.

LIST OF TABLES

Table	Title	Page
4.1	Eigenvalues computed from stiffness matrix of SFCNQ.....	34
4.2	Normalised tip displacements from MacNeal – Harder thin cantilever beam test under shear load.	36
4.3	Normalised stresses from MacNeal – Harder thin cantilever beam test under shear load	36
4.4	Normalised tip displacements from MacNeal – Harder thin cantilever beam test under extension load	37
4.5	Normalised stress from MacNeal – Harder thin cantilever beam test under shear load.....	37
4.6	Normalised tip displacements for thin deep cantilever beam ($l/h = 100$)	38
4.7	Normalised tip displacements for thick deep cantilever beam ($l/h = 5$).....	39
4.8	Tip displacements and average stresses computed from constant strain patch test.....	44
4.9	Average stresses obtained in weak patch test.....	46
5.1	Eigenvalues computed from stiffness matrix of SFCSS	49
5.2	Single element aspect ratio sensitivity test.....	50
5.3	Normalised tip displacements of a slender beam under shear load.....	51
5.4	Normalised stresses (σ_{xx}) at the root of a slender beam under shear load ...	52
5.5	Normalised tip displacements of a slender beam under extension load.....	53
5.6	Normalised stresses (σ_{xx}) at the root of a slender beam under extension load.....	53
5.7	Tip displacements from constant strain patch test	57
5.8	Average stresses (σ_{xx}) from constant strain patch test.....	57
5.9	Stresses at different points from weak patch test	58
5.10	Results from Boussinesq problem of cylindrical volume	60
6.1	Eigenvalues computed from stiffness matrix of SFCFP	64

LIST OF FIGURES

Figure	Title	Page
3.1	SFCNQ Element Geometry.....	19
3.2	SFCSS Element Geometry.....	22
3.3	SFCFP Element Geometry.....	25
3.4	Schematic flow diagram of the software.....	27
4.1	Eigenvalue test model using single element.....	34
4.2	MacNeal – Harder thin cantilever beam.....	35
4.3	Deep cantilever modelled with rectangular element.....	38
4.4	Two element distortion sensitivity test.....	39
4.5	Distortion sensitivity test - Percentage error in tip displacements Vs Magnitude of geometric distortion.....	40
4.6	Infinite plate with a cut out at the centre.....	41
4.7	Stress computed along the edge AB of an infinite plate with a discontinuity at the centre.....	42
4.8	Circular disc with concentrated edge load.....	42
4.9	Stress distribution along the diameter of the circular disc with concentrated edge load.....	43
4.10	Element mesh for constant strain patch test.....	44
4.11	Element mesh for weak patch test.....	45
5.1	Eigenvalue test model using single element.....	48
5.2	Aspect ratio sensitivity test.....	50
5.3	MacNeal - Harder slender beam test.....	51
5.4	Two element distortion sensitivity test using deep beam.....	54
5.5	Two element distortion sensitivity test for tip displacement under shear load.....	55
5.6	Two element distortion sensitivity test for stress under shear load.....	55
5.7	Two element distortion sensitivity test for tip displacement under bending load.....	55

5.8	Two element distortion sensitivity test for stress under bending load	56
5.9	Element mesh for constant strain patch test	56
5.10	Weak patch test - element geometry	58
5.11	Finite element model for Boussinesq problem for cylindrical volume	59
5.12	Element mesh for Curved shell test.....	60
5.13	Convergence curve for the spherical shell test.....	61
6.1	Eigenvalue test model using single element.....	64
6.2	Single element results, twist case using differential loads	65
6.3	Rectangular plate structure parameters for convergence test	66
6.4	Quarter plate finite element models	67
6.5	Convergence results for a simply supported plate with a central point load and aspect ratio one	68
6.6	Convergence results for a simply supported plate with a central point load and aspect ratio two	68
6.7	Convergence results for a simply supported plate with a central point load and aspect ratio three	69
6.8	Convergence results for a clamped plate with a central point load and an aspect ratio one	69
6.9	Convergence results for a clamped plate with a central point load and an aspect ratio two	70
6.10	Convergence results for a clamped plate with a central point load and an aspect ratio three	70

NOTATIONS

Mathematical symbols

$[\]$	-	Rectangular or square matrix
$\{ \}$	-	Column, row and diagonal matrices
$[\]^T$	-	Matrix transpose
$[\]^{-1}$	-	Matrix inverse

Latin symbols

$a_1, a_2, \dots, b_1, b_2, \dots, c_1, c_2, \dots$		Coefficients of polynomial terms
B_x, B_y, B_z	-	Body forces in x, y and z directions
D	-	$E/(1-\nu^2)$
D_1	-	$E t^3/12(1-\nu^2)$
D_2	-	$E t^3/24(1+\nu)$
E	-	Modulus of elasticity
G	-	Shear modulus
$[K], [k]$	-	Global and elemental stiffness matrices
t	-	Thickness of the material
u, v, w	-	Translations along x, y and z directions.
$\{u\}$	-	Vector of displacements; $\{u\} = [u \ v \ w]^T$

Greek symbols

$\epsilon_x, \epsilon_y, \epsilon_z$	-	Linear strains in x, y and z directions
$\epsilon_{xy}, \epsilon_{xz}, \epsilon_{yz}$	-	Shear strains in xy, xz and yz planes
λ	-	$E\nu/(1+\nu)(1-2\nu)$
ν	-	Poisson's ratio of an isotropic material
$\sigma_x, \sigma_y, \sigma_z$	-	Direct stresses in x, y and z directions
$\sigma_{xy}, \sigma_{xz}, \sigma_{yz}$	-	Shear stresses in xy, xz and yz planes

CHAPTER 1

INTRODUCTION

1.1 Motivation

The development of finite element method (FEM) as an analysis tool for continuum problems coincided with arrival of powerful digital computers. Using this method it is possible to establish and solve equations pertaining to complex systems in a very simple manner. The simplicity with which intricate structures can be represented and analysed on the computers has made FEM a versatile and widely applied method for both analysis and design of structures.

Subsequent to the development of the finite element method, research efforts have been targeted at improving the performance of elements and developing specialised elements to meet specific applications. As a consequence, many commercial finite element packages with built-in element libraries and capabilities to deal with a wide range of problems have been developed. Even with these improvements, researchers are still in the search for simple elements, which can give accurate estimates of structural response with minimum computational effort. Higher order elements or elements based on other variational principles are capable of accurate modelling of structural behaviour. However, simpler elements based on principle of minimum potential are preferable. This preference is mirrored in the concentration of research efforts on techniques to improve the lower order elements. Such techniques would be more appealing if they could be extended to higher order elements as well.

Considerable research efforts have been made to develop such elements for plane stress, plate bending and three dimensional problems. Consequently, a number of

lower order elements like four noded quadrilateral for plane stress analysis, sixteen noded brick element for three dimensional analysis etc., have been developed. Even though these elements are simpler and consequently very popular, a large number of these elements have to be used to obtain reasonably accurate solutions. When problems of in-plane bending are considered, the element gets affected by parasitic shear and when very thin beams are modelled using these conventional elements, the beam locks and refuses to bend.

A number of techniques like reduced or selective integration, introduction of incompatible or bubble modes, subdividing the elements and averaging shear computed in the subdivisions, assuming stress or strain distributions with constant shear, hybrid or mixed method approaches, introduction of drilling degrees of freedom etc., have been suggested to improve the performance of these elements by alleviating the parasitic shear effect. Most of these techniques are extendable to higher order elements as well and in fact, difficulties of modelling other problems such as near incompressible volumetric analysis and plate and shell behaviour have been overcome by using extension of these techniques.

However these techniques are effective only to a certain extent, each one has its own inadequacies. Even though they decrease the susceptibility of the element to parasitic shear effects, it is accomplished by considerable manipulation of the assumed displacement functions. Such techniques are known as “extra-variational”, (Strang and Fix 1972) as these are extraneous to the variational principle on which the mathematical model is based. Even with these improvements some elements fail to perform well under certain loading conditions with arbitrary element shape and hence

need further improvements. A more direct and justifiable approach is required and the work presented in this thesis presents such an approach.

An approach that can probably overcome many of these problems would be to consider elements in which the assumed displacement functions satisfying the differential equations of stress field equilibrium. Such a method not only have equilibrium between elemental forces (in an integrated sense) and applied loads at the nodes of the structure, but also have the stress fields within each element in equilibrium individually. Such elements are likely to give better solutions than the existing elements. In the present work, efforts have been made to develop field equilibrium finite elements for the analysis of two and three dimensional elasticity and plate bending problem.

1.2 Layout

Chapter 1 explains the motivation of the research work and a brief description of the layout of the thesis. Chapter 2 contains a brief review of the important lower order finite element formulations for two dimensional, three dimensional and plate bending analyses, developed in the last three decades. In addition, a representative sample of extra-variational techniques currently in use, are included. Chapter 3 contains a general procedure for developing displacement functions that satisfy differential equations of stress field equilibrium. Using this procedure, the displacement functions and stiffness matrices for a nine node quadrilateral plane stress element, a sixteen node brick element for three dimensional stress analysis and a four node plate bending element have been generated. Development of computer programs for numerical implementation of these elements is also outlined. In chapter 4, 5 and 6 numerical investigations on the performance of these elements have been carried out through

standard test problems for validation purpose. Chapter 7 contains a summary of the work and few remarks to emphasise the scope of this study. Appendices 1 and 2 contain the required constraint equations, for the formulation of nine node plane stress element and sixteen node three dimensional element respectively.

CHAPTER 2

LITERATURE REVIEW

2.1 General

The finite element method today, has become a powerful tool in engineering analysis and design. The ease of application, reliability of solutions and ability to model complex geometries seem to be the main reasons for its popularity. It encompasses many diverse fields like structural mechanics, fluid mechanics, solid mechanics, electromagnetism etc.

Like in all original developments it is difficult to pin point an exact date for the initiation of finite element method. Basic ideas of the FEM originated from advances in aircraft structural analysis. The development of FEM mainly attributed to three separate groups- mathematicians (Courant 1943, Collatz 1950, Courant and Hilbert 1953), physicists (Synge 1957) and engineers (Turner *et al.*1956). Courant's paper, which used piecewise polynomial interpolation over triangular sub regions to model torsion problems, appeared in 1943. The term *finite element* was first used by Clough (1960). In the late 1960's and early 1970's, finite element analysis was applied to non-linear problems and large deformations. Mathematical foundations were laid in the 1970's. New element development, convergence studies and other related areas fall in this category.

A comprehensive study on the historical development of the family of finite element can be made by broadly classifying it in to conforming and nonconforming elements.

2.2 Development of conforming finite elements

Conforming elements are formulated by strictly adhering to the three cardinal principles, known as “convergence criteria” (Zienkiewicz and Taylor 1989). Conventionally, to ensure convergence to the exact solution, the interpolation function should satisfy certain criteria. They are formally defined as given below.

- a. The displacement function must be continuous within the element. One way of satisfying this condition is by choosing complete polynomials for the displacement model.
- b. The displacement function must be capable of representing rigid body displacement of the element. The constant terms in the displacement polynomial would ensure this condition.
- c. The displacement function must be capable of reproducing the exact strain states defined by the respective elasticity equations within the element. In one, two and three dimensional elasticity problems, the linear terms in the assumed displacement function would satisfy this requirement. In the case of beam, plate and shell element the displacement function should be capable of representing constant curvature states.

Conventional finite elements also satisfy compatibility conditions. The displacements must be compatible between adjacent elements. When the elements deform, there must not be any discontinuity like overlap or separation between the elements. In the case of beam, plate and shell element, this requirement would ensure that there should not be any discontinuity or sudden changes in slope across the inter-element boundaries. Elements that satisfy the convergence requirements and compatibility conditions are called Conforming elements. And elements, which violate

compatibility conditions, but satisfy the convergence requirements, are termed as Nonconforming elements.

It will be Herculean to list all the conforming elements developed so far. Hence only a few of them, which can be treated as milestones in the development of conforming elements, are considered here. The literature review is presented here under the subtitle two-dimensional and three-dimensional finite elements and plate elements.

2.2.1 Two dimensional and three dimensional finite elements

From early days, major research efforts have been made to develop simpler and lower order finite elements with translational degrees of freedom only, like four node quadrilateral used in two-dimensional analysis, eight node brick element and simple tetrahedral element in three dimensional analysis. The four node quadrilateral element QUAD4 (Zienkiewicz and Taylor 1989, Cook *et al.* 1989) which is a bilinear isoparametric element used for plane stress analysis is one of the simplest element. Hence this element is used as a 'work horse' element in most of the applications. The only draw back is that a very fine mesh is required to get reasonably accurate solutions. This is especially true when problems with in-plane bending loads are modelled. More over shear stress predicted across the element oscillates enormously. Even prior to this element, a quadrilateral element built with four constant strain triangles had been developed (Cook 1969, Cook *et al.* 1989). The internal node was condensed out and stress was evaluated at the centre of the quadrilateral using an averaging scheme. However this element was also affected with parasitic shear and the performance was slightly inferior to the QUAD4 (Desai and Abel 1972)

The first formulation of simple tetrahedral element was done by Gallagher *et al.* (1962) and they used it for stress analysis of heated complex shapes. Early elaborations

of tetrahedral elements were by Melosh (1963 a.) and Clough (1969). An extensive numerical study was done by Rashid *et al.*(1969 b. and 1970). These elements used volume co-ordinates similar to triangular elements that used area co-ordinates, and were simple generalisation of the later. Amongst them the first (Gallagher *et al.* 1962) was a C^0 continuous, 4 node, 12 dof constant strain tetrahedron. It used linear shape functions along the three orthogonal cartesian directions.

Clough (1969) used a C^0 , 10 node, 30 dof linear strain tetrahedron by adding mid-side nodes. This tetrahedron used complete quadratic polynomials in the three directions. Rashid *et al.*(1969 a.) used a C^0 , 16 node, 48 dof tetrahedron. Hughes and Allik(1969) have formulated and used a 4 node 48 dof tetrahedron. They used four vertex nodes and dof of u, v, w and their derivatives in x, y, z, directions at each node. Being a higher order element with derivative degree of freedom, it required higher order continuity. As it could be expected "this is the most advantageous tetrahedron introduced"(Yang 1986). Initial work on conforming hexahedral elements were restricted to rectangular ones. Since the faces and sides of the rectangular elements are orthogonal to one another, these elements can be formulated using non-dimensional local co-ordinate systems. Many such elements are available. Amongst the first was a C^0 , 8 node, 24 dof, linear displacement, rectangular tetrahedron (Melosh 1963 b., Clough 1969). The element used tri-linear displacement interpolation functions in the three orthogonal directions. The addition of one node to midpoint of each side gives a C^0 , 20 node, 60 dof, and quadratic displacement hexahedron. Like tri-linear element used incomplete cubic polynomials, this element used incomplete quadratic ones.

The addition of four facial nodes and eight interior nodal points yield a 54 node, 192 dof, C^0 hexahedral element first used by Argyris and Fried (1968). Here the

interpolation functions are obtained by taking the product of three complete cubic polynomials in three directions. Another commonly used rectangular Lagrangian element is from the use of the product of quadratic polynomials in the three orthogonal directions. It is a 27 node, 54 dof hexahedron with a centroidal node, the degree of freedom corresponding to this could be statically condensed. The Lagrangian element has a disadvantage that the interpolation functions require the use of large degrees of polynomial. Solid finite elements of shape other than tetrahedron or hexahedron are also available. Some of them are wedge shaped and pentagonal elements. For wedge shaped elements (triangular prisms) the interpolation functions are obtained as the product of Lagrange approach and Serendipity approach.

In the elements described above the number of nodes has to be increased to increase the order of the interpolation polynomial. Alternatively, the elements with higher derivatives of displacements as nodal degrees of freedom can also be used. Another means of generating interpolating functions is to use hierarchic approximations. Here one needs to associate the monomial term in each interpolating polynomial with just a parameter and not to one with an obvious physical meaning. Further hierarchic functions need to have zero values at the end of the range (on the nodal points along each edge under consideration). Using these polynomials one can arrive at a variety of interpolation functions for elements of different geometries.

2.2.2 Plate elements

Problems involving thick plates consist of complete set of three-dimensional differential equations and have to be tackled with solid finite elements. Thin plates with small deflections can be dealt with noncompatible finite elements based on Kirchhoff's theory of thin plates in which the transverse shear deformations are

neglected. Several attempts have been made in the past to develop simple and efficient plate elements using displacement models satisfying the C^0 continuity requirement. These models are based on Mindlin theory, which considers shear deformation in plates. In C^0 continuous elements, three independent displacement quantities namely w , θ_x and θ_y are to be considered for the inclusion of shear deformation. Hence for the finite element formulation, three shape functions are chosen to represent the variation of w , θ_x and θ_y . Such elements showed promise for application to thick or thin plates, with curved boundaries. However, main difficulty experienced in the use of such elements was that they experienced over stiff locking behaviour in thin plate situations. Zienkiewicz *et al*(1971) proposed an eight node isoparametric element with reduced integration, capable of using in the thin plate situations.

Another approach to the development of elements for thin plates involves the use of discrete Kirchhoff theory(Bathe *et al.* 1980, Bathe 1982). In this approach, the independent displacement quantities were assumed for the finite element formulation of w , θ_x and θ_y , and only C^0 continuity requirements need to be satisfied. The transverse shear energy is neglected and Kirchhoff hypothesis is introduced in a discrete way along the edges of the element to relate the rotations to the transverse displacements. Hence the constraint of zero shear strain ($\gamma_{xz} = \gamma_{yz} = 0$) is imposed at the discrete number of points along the edges of the element to represent the behaviour of the thin plates. Each constraint removes one degree of freedom and thus yields a flexible mesh. This property makes it possible to avoid element locking associated with the lower order elements applied to very thin plates. The implementation of DKT(Discrete Kirchhoff Triangle) is complicated and the elements predict stresses relatively poorly.

2.3 Development of nonconforming finite elements

Elements mentioned so far were derived by strictly adhering to the convergence criteria. The behaviour of these elements in situations, such as bending or near incompressibility limit (especially the lower order elements) are not very encouraging. The reasons for the poor performance of these elements are mainly due to parasitic locking and incompressibility locking. The term locking is used to denote a definite decay of accuracy in displacement recovery. Other common problems encountered are “violent stress oscillations” (Prathap 1992) and delayed convergence. Various new elements formulated lately, address themselves to tackle these problems. Since the early days, the development of such elements has been the source of both challenge and motivation for new developers.

2.3.1 Two dimensional and Three dimensional elements

Many techniques do exist in the literature to tackle the above-mentioned problems. Many of these techniques are categorised as “ad hoc”, for their success in some problems does not necessarily imply the same when extrapolated to other problems. These techniques are the “milestones” of progress of FEM and are called extra variational techniques (MacNeal 1992). A few of them worked very well in certain situations but failed in other situations. The important techniques that developed over the years for the improvement of the performance of these finite elements are described in subsequent sections.

2.3.1.1 Reduced or selective integration

This method is applicable to all types of finite elements such as two dimensional, three-dimensional and plate elements. Here the strain energy is not exactly integrated.

An 'n' point rule in one dimension can be used to integrate a polynomial of the order $2n - 1$ exactly (Conte and de Boor 1980). Usage of a lower Gauss point rule than that is required for exact integration of the strain energy will result in reduced integration and faster convergence to the exact solution. In selective integration, the different strain energy terms are integrated with different order of integration (Hughes, Taylor and Kanoknukulchai 1977).

These rules need to be used with care. A very low order integration can lead to mechanisms, while the use of a very high order leads to delayed convergence. One common mechanism encountered during reduced integration is the presence of hourglass modes. Zeinkiewicz and Taylor (1989) proved that for success of this method the gauss points selected should be exactly the optimal points for the stress recovery.

2.3.1.2 Addition of bubble modes

The technique involves the addition of certain degrees of freedom not associated with any node (Wilson 1973). This brought into use, incompatible elements, where the displacement fields are not continuous across element boundaries. The variables associated with the nodeless degrees of freedom are later condensed out.

MacNeal (1987) proved analytically that it is impossible for a rectangular element with only four nodes to be able to model in-plane bending satisfactorily and also to pass patch test. This difficulty has to be overcome either by introducing incompatible modes or by increasing the number of degrees of freedom in the transverse direction on the model. Wilson *et al.* (1973) introduced the incompatible element Q6. This element has additional degrees of freedom, which are incompatible and popularly known as 'bubble modes'. Static condensation is necessary and it is found that the

resulting element has to be further manipulated with selective integration of the incompatible or bubble modes in order for it to pass the patch test. Taylor *et al.*(1976) developed the approach for making the Q6 to pass the patch test and called the element QM6. The element QM6 is not susceptible to parasitic shear and also performs well in other situations. However this element also experiences difficulties when modelling in-plane bending using increasingly distorted or quadrilateral meshes. The eight-node brick element when used in tandem with reduced integration, gives very good results. It has found its way into many commercial finite element packages. Unfortunately use of these techniques requires expertise. The polynomial functions so chosen to represent the nodeless degrees of freedom should be the exact ones required for eliminating the required type of locking. For example, in the eight-node brick element, the incompatible modes selected alleviate the parasitic shear.

2.3.1.3 Using unequal order of interpolation

This is a simple technique in use, especially for one and two-dimensional elements. Here the order of the interpolation functions used for the rotational degrees of freedom are one less than that used for the translational ones. Its success could be attributed to the terms dropped from the interpolation functions of the rotational degrees of freedom. They are exactly the one, which if present will cause locking. Unequal order of interpolation has been used in the formulation of the many finite elements. For example, Tessler and Dong (1981) formulated one such Timoshenko beam element.

2.3.1.4 Assumed strain method

This technique involves the use of interpolation functions of lower order and smoothening them in some least square sense (MacNeal 1982). The method has an advantage that the procedure can be used to obtain the interpolation function.

2.3.1.5 Residual energy balancing

Here certain constraints contributing to locking are identified. They are then artificially removed by using a constant, which the designer of the element sets an arbitrarily small value (Fried 1975, Cook 1977). The value of the constant is problem dependent and it is difficult to choose one value for a set of elements or problems. The constant is also mesh dependent, by that increasing the confusion. Stresses predicted by this method are “very unreliable” (Prathap 1992) and grossly depend on the scaling constant chosen.

2.3.1.6 Other general methods

Amongst the most popular formulations are the one in which compatible displacements and equilibrating stresses are independently formulated. Stress parameters are eliminated at the element level (Pian 1973). These formulations are known as hybrid/mixed formulations. Many three dimensional hybrid/mixed stress elements have been developed (Zienkiewicz and Taylor 1989). Here too, extravariational techniques like reduced integration and introduction of bubble modes can be used. Other elements formulated using these principles are eight node elements (Irons 1972), 20-node element (Ahmad and Iron 1974), special purpose three dimensional elements for thick plate analysis (Spilker 1981). Tang and Chen (1982) proposed a series of nonconforming stress based elements. Chen and Cheung (1987) derived a new functional (a functional with displacements, stresses and strains as independent variables) to obtain a series of isoparametric elements. Sze and Ghali (1993) started with assumed stress element and identified the strain components that cause locking and selectively scale them down to obtain an incompatible element.

There are several other ingenious techniques used to obtain better elements. Some of them are synthesis using Fourier components (Park 1984), use of trigonometric interpolation functions (Heppler and Hanson 1987) etc.

Another technique developed by Prathap (1986 and 1992), says that in-plane bending involving Kirchhoff constraint of zero shear energy in very thin beams is a constrained minimal problem. It is not possible to model these constraints directly to a displacement based finite element. Instead, a displacement field that is consistent with the constraints has to be used. This is accomplished by identifying the term in the expression for shear strain that absorbs parasitic energy and ignoring the contribution of that term during shear energy computation. The consistent field principle is a technique that is applicable to any constrained minimal problem such as plate bending and near incompressible three-dimensional analysis. Unfortunately this technique cannot be applied to any arbitrary quadrilateral (Prathap 1992). However, this technique throws more light on the locking problem.

All the techniques summarised above are artifices, attempted to primarily deal with the locking effect. Moreover, each technique has its own risk and inadequacies and often needs further manipulation of elemental functions to enable it to perform well in all loading situations.

2.3.2 Plate elements

A variety of plate elements have been proposed since the early days of finite element. The development of plate bending element based on Kirchhoff's theory of thin plates lead to either incompatible elements or involved complicated formulation and programming (Zienkiewicz and Taylor 1991). A rectangular plate element with 12 dof proposed by the Melosh (1963 c.) is one of the oldest and best known element. This

element has three dof w , $\partial w/\partial x$, and $\partial w/\partial y$ per node and is not fully compatible. However the performance of the element is reasonably good and is widely used (Zienkiewicz and Taylor 1991). Bogner, Fox and Schmit (1965) developed a sixteen degrees of freedom element (LCCT-12). Clough and Felippa (1968) proposed a refined quadrilateral element in which a sub domain approach is used. Although the LCCT-12 element employs an optimum compatible displacement field, its midside node and rotational degrees of freedom complicate the analysis. A special version of this element designated as LCCT-11 is developed by avoiding the midside node, employs the static condensation of the internal degrees of freedom. This element is a fully compatible element and gave good results in the analysis of plate bending.

2.4 Test problems for element performance comparisons

All the elements mentioned above, have tested with standard test problems and the results were compared with that obtained with other similar elements. Comparisons are generally made against standard problems proposed in the literature (MacNeal and Harder 1985, White and Abel 1989). They include a variety of problems such as patch tests, problems with in-plane bending, problems with stress concentration, curved shell tests, three dimensional tests etc.

These tests were considered to indicate the performance of the element in general. It has been observed that no single element is capable of performing well in all these problems. The most common failing of these occurs when increasingly distorted meshes are used in models involving in-plane bending.

2.5 Scope of the present work

After detailed review of the literature, definite need is felt for exploring the possibilities of finite element that will not have the deficiency of locking and related

drawbacks. This thesis addresses the development of field equilibrium finite elements and proposing them for the stress analysis of membranes, solids and thin plates. Field consistent approach is based on displacement functions that satisfies stress equilibrium equations and hence combines the simplicity of displacement formulation and accuracy in stress prediction.

A new family of elements within which the displacement functions satisfy the differential equations of stress field equilibrium are proposed for the plane stress, three dimensional and plate bending analysis. The objectives of the thesis are listed below.

- Development of a general procedure to construct displacement polynomials which satisfy the differential equations of stress field equilibrium for plane stress, three dimensional and plate bending elements.
- Generation of elemental stiffness matrices of simple plane stress, three dimensional and plate bending elements using the above procedure.
- Development of Software for implementation of these elements.
- Testing the performance of these elements on standard test problems and comparing the results with theoretical closed form solutions and results obtained with other existing elements.

CHAPTER 3

DEVELOPMENT OF FIELD EQUILIBRIUM

FINITE ELEMENTS

3.1 General

Field equilibrium finite elements, which are based on displacement functions that satisfy the differential equations of stress field equilibrium, are presented in this chapter. A general procedure, for constructing the displacement functions, which satisfy equilibrium at every point inside the element and the generation of stiffness matrices using field equilibrium approach, is described. A nine node quadrilateral element for plane stress analysis, a sixteen node solid element for three dimensional stress analysis and a four node quadrilateral element for plate bending analysis have been developed and explained subsequently. Software for the implementation of the finite elements is outlined.

3.2 Generation of plane stress element

3.2.1 Displacement functions

A nine-node quadrilateral element with two degrees of freedom per node is considered. The element is referred to by the acronym - *SFCNQ* – Stress Field Consistent Nine Node Quadrilateral, in further discussions. Generation of displacement functions of SFCNQ consists of the following steps.

Step 1. Complete quartic polynomials in x and y, with 30 unknown coefficients are considered to interpolate the displacements **u** and **v** of the element.

$$\begin{aligned} u = & a_1 + a_2x + a_3y + a_4x^2 + a_5xy + a_6y^2 + a_7x^3 + a_8x^2y + a_9xy^2 + a_{10}y^3 + a_{11}x^4 + a_{12}x^3y \\ & + a_{13}x^2y^2 + a_{14}xy^3 + a_{15}y^4 \end{aligned} \quad (3.1a)$$

$$v = b_1 + b_2x + b_3y + b_4x^2 + b_5xy + b_6y^2 + b_7x^3 + b_8x^2y + b_9xy^2 + b_{10}y^3 + b_{11}x^4 + b_{12}x^3y + b_{13}x^2y^2 + b_{14}xy^3 + b_{15}y^4 \quad (3.1b)$$

Step 2. The stress field equilibrium equations for two dimensional analysis are as follows.

$$\frac{\partial \sigma_x}{\partial x} + \frac{\partial \sigma_{xy}}{\partial y} = 0 \quad (3.2a)$$

$$\frac{\partial \sigma_y}{\partial y} + \frac{\partial \sigma_{xy}}{\partial x} = 0 \quad (3.2b)$$

Using strain displacement relations and stress strain relations for plane stress conditions, the equations of stress field equilibrium are rewritten as

$$D \left[\frac{\partial^2 u}{\partial x^2} + \nu \frac{\partial^2 v}{\partial x \partial y} \right] + G \left[\frac{\partial^2 u}{\partial y^2} + \frac{\partial^2 v}{\partial x \partial y} \right] = 0 \quad (3.3a)$$

$$D \left[\frac{\partial^2 v}{\partial y^2} + \nu \frac{\partial^2 u}{\partial x \partial y} \right] + G \left[\frac{\partial^2 v}{\partial x^2} + \frac{\partial^2 u}{\partial x \partial y} \right] = 0 \quad (3.3b)$$

Where $D = E/(1-\nu^2)$ and $G = E/2(1+\nu)$

Step 3. The displacement polynomials (eqn.3.1) are substituted in eqn. 3.3 and the constraint equations in terms of unknown coefficients ($a_1, \dots, a_{15}, b_1, \dots, b_{15}$) are extracted. These equations are listed in appendix 1.

Step 4. Originally 30 unknown coefficients were associated with the assumed displacement polynomial of the element. By virtue of the twelve constraint equations, the unknowns associated with an element reduce to eighteen only.

3.2.2 Element geometry

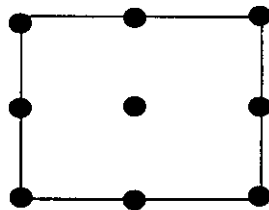


Fig. 3.1 SFCNQ - Element Geometry

The geometry of Stress Field Consistent Nine Node Quadrilateral Plane Stress Element (*SFCNQ*) is given in fig.3.1. The element has four corner nodes, four mid-side nodes and an internal node. Each node has two degrees of freedom, namely u and v in x and y co-ordinate directions respectively.

3.3 Generation of three dimensional element

3.3.1 Displacement functions

A sixteen-node solid element with three degrees of freedom per node is considered. The element is referred to by the acronym - *SFCSS* – Stress Field Consistent Sixteen Node Solid element, in further discussions. Generation of displacement functions of *SFCSS* consists of the following steps.

Step 1. Complete cubic polynomials in x, y and z with 60 unknown coefficients are considered to interpolate the displacements **u** , **v** and **w** of the element.

$$u = a_1 + a_2x + a_3y + a_4z + a_5x^2 + a_6yx + a_7zx + a_8y^2 + a_9zy + a_{10}z^2 + a_{11}x^3 + a_{12}x^2y + a_{13}xy^2 + a_{14}y^3 + a_{15}x^2z + a_{16}xz^2 + a_{17}y^2z + a_{18}yz^2 + a_{19}xyz + a_{20}z^3 \quad (3.4a)$$

$$v = b_1 + b_2x + b_3y + b_4z + b_5x^2 + b_6yx + b_7zx + b_8y^2 + b_9zy + b_{10}z^2 + b_{11}x^3 + b_{12}x^2y + b_{13}xy^2 + b_{14}y^3 + b_{15}x^2z + b_{16}xz^2 + b_{17}y^2z + b_{18}yz^2 + b_{19}xyz + b_{20}z^3 \quad (3.4b)$$

$$w = c_1 + c_2x + c_3y + c_4z + c_5x^2 + c_6yx + c_7zx + c_8y^2 + c_9zy + c_{10}z^2 + c_{11}x^3 + c_{12}x^2y + c_{13}xy^2 + c_{14}y^3 + c_{15}x^2z + c_{16}xz^2 + c_{17}y^2z + c_{18}yz^2 + c_{19}xyz + c_{20}z^3 \quad (3.4c)$$

Step 2. For three dimensional stress analysis of a homogeneous isotropic material, the kinematic strain displacement relations are as given by eqn 3.5

$$\epsilon_x = \frac{\partial u}{\partial x} \quad (3.5a)$$

$$\epsilon_y = \frac{\partial v}{\partial y} \quad (3.5b)$$

$$\epsilon_z = \frac{\partial w}{\partial z} \quad (3.5c)$$

$$\epsilon_{xy} = \frac{\partial u}{\partial y} + \frac{\partial v}{\partial x} \quad (3.5d)$$

$$\epsilon_{xz} = \frac{\partial u}{\partial z} + \frac{\partial w}{\partial x} \quad (3.5e)$$

$$\epsilon_{yz} = \frac{\partial v}{\partial z} + \frac{\partial w}{\partial y} \quad (3.5f)$$

The constitutive relations for a homogeneous isotropic material are given in eqn.3.6

$$\sigma_{xx} = (\lambda + 2G) \epsilon_x + \lambda(\epsilon_y + \epsilon_z) \quad (3.6a)$$

$$\sigma_{yy} = (\lambda + 2G) \epsilon_y + \lambda(\epsilon_x + \epsilon_z) \quad (3.6b)$$

$$\sigma_{zz} = (\lambda + 2G) \epsilon_z + \lambda(\epsilon_x + \epsilon_y) \quad (3.6c)$$

$$\sigma_{xy} = G \epsilon_{xy} \quad (3.6d)$$

$$\sigma_{xz} = G \epsilon_{xz} \quad (3.6e)$$

$$\sigma_{yz} = G \epsilon_{yz} \quad (3.6f)$$

Where $\lambda = \frac{E\nu}{(1+\nu)(1-2\nu)}$ and $G = \frac{E}{2(1+\nu)}$

The equations of equilibrium for three dimensional problem are given in eqn.3.7.

$$\frac{\partial \sigma_x}{\partial x} + \frac{\partial \sigma_{xy}}{\partial y} + \frac{\partial \sigma_{xz}}{\partial z} + B_x = 0 \quad (3.7a)$$

$$\frac{\partial \sigma_y}{\partial y} + \frac{\partial \sigma_{xy}}{\partial x} + \frac{\partial \sigma_{yz}}{\partial z} + B_y = 0 \quad (3.7b)$$

$$\frac{\partial \sigma_z}{\partial z} + \frac{\partial \sigma_{xz}}{\partial x} + \frac{\partial \sigma_{yz}}{\partial y} + B_z = 0 \quad (3.7c)$$

Where B_x , B_y and B_z are the body forces. Terms defined by eqn.3.5 are substituted in constitutive relations (eqn.3.6). The stress value in this modified form is substituted in equilibrium equations. The modified equilibrium equations are given in eqn.3.8

$$(\lambda + G) \left[\frac{\partial^2 u}{\partial x^2} + \frac{\partial^2 v}{\partial x \partial y} + \frac{\partial^2 w}{\partial x \partial z} \right] + G \left[\frac{\partial^2 u}{\partial x^2} + \frac{\partial^2 u}{\partial z^2} + \frac{\partial^2 u}{\partial y^2} \right] = 0 \quad (3.8a)$$

$$(\lambda + G) \left[\frac{\partial^2 v}{\partial y^2} + \frac{\partial^2 u}{\partial x \partial y} + \frac{\partial^2 w}{\partial y \partial z} \right] + G \left[\frac{\partial^2 v}{\partial y^2} + \frac{\partial^2 v}{\partial x^2} + \frac{\partial^2 v}{\partial z^2} \right] = 0 \quad (3.8b)$$

$$(\lambda + G) \left[\frac{\partial^2 w}{\partial z^2} + \frac{\partial^2 u}{\partial x \partial z} + \frac{\partial^2 v}{\partial y \partial z} \right] + G \left[\frac{\partial^2 w}{\partial z^2} + \frac{\partial^2 w}{\partial x^2} + \frac{\partial^2 w}{\partial y^2} \right] = 0 \quad (3.8c)$$

It is rewritten with the displacement functions given in eqn. 3.4. The resulting polynomial expressions should vanish at all points within the element. This is possible only if the coefficient of each polynomial term vanishes individually. Since the polynomials considered in eqn. 3.4 are limited to third order, twelve constraint equations on the unknown coefficients are obtained. These constraint equations are listed in appendix 2.

Step 3. The assumed polynomials with 60 unknowns can be expressed with reduced number of unknown coefficients(48) using these twelve constraint equations. Thus a 16 noded brick element with 3 dof per node (element dof is 48) is sufficient for incorporating third order displacement polynomials. This sixteen noded brick element has three degrees of freedom u, v, and w at each node and is shown in fig. 3.2. Innovatively, various other element geometries and node distributions can be considered for accommodating various degrees of displacement polynomials.

3.3.2. Element geometry

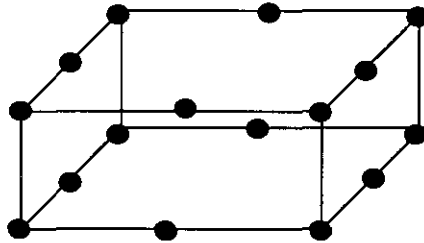


Fig. 3.2 SFCSS - Element Geometry

The geometry of Stress Field Consistent Sixteen Node Solid Element(*SFCS5*) is given in fig.3.2. The element has eight corner nodes, eight mid-side nodes. Each node has three degrees of freedom, namely u, v and w in x ,y and z co-ordinate directions respectively.

3.4 Generation of plate bending element

3.4.1 Displacement functions

Following the same procedure used in the other two cases, different possible combinations of element shapes and node distributions are tried using complete interpolation polynomials. But the method fails to develop simple plate elements with conventional and understandable degrees of freedom. Hence the possibility of adopting interpolation polynomial from an existing element is examined. A four noded quadrilateral element with three degrees of freedom $w, \partial w/\partial x, \partial w/\partial y$ per node (element dof is 12) is considered. The element is referred to by the acronym - *SFCFP* – Sress Field Consistent Four Node Plate element.

Step 1. ‘Complete polynomial’ (Bogner *et al.* 1965) in x and y with 16 unknown coefficients are considered to interpolate the w displacement of the element.

$$w = a_1 + a_2x + a_3y + a_4x^2 + a_5xy + a_6y^2 + a_7x^3 + a_8x^2y + a_9xy^2 + a_{10}y^3 + a_{11}x^3y + a_{12}x^2y^2 + a_{13}xy^3 + a_{14}x^3y^2 + a_{15}x^2y^3 + a_{16}x^3y^3 \quad (3.9)$$

This interpolation function was first used by Bogner *et al.*(1965) in a four noded quadrilateral plate element with four dof per node, namely $w, \partial w/\partial x, \partial w/\partial y$ and $\partial^2 w/\partial x \partial y$. The above polynomial is a ‘complete polynomial’ for the terms of expression corresponds to the product $(1+x+x^2+x^3)(1+y+y^2+y^3)$. This displacement

function results in a cubic polynomial for displacements and slopes along the edges of the element.

Step 2. The stress field equilibrium equations for plate bending analysis is given in eqn.3.10

$$\frac{\partial^2 M_x}{\partial x^2} + \frac{\partial^2 M_y}{\partial y^2} + \frac{2\partial^2 M_{xy}}{\partial x \partial y} = 0 \quad (3.10)$$

Using the strain displacement relations (Curvature -Vertical displacement relationship) and stress strain relations (Moment - Curvature relationship), the equations of stress field equilibrium are rewritten as

$$\frac{\partial^4 w}{\partial x^4} + \frac{\partial^4 w}{\partial y^4} + \frac{2\partial^4 w}{\partial x^2 \partial y^2} = 0 \quad (3.11)$$

Step 3. The displacement polynomial (eqn.3.9) are substituted in eqn. 3.11 and the constraint equations in terms of unknown coefficients(a_1, \dots, a_{16}) are extracted. These equations are given in eqn. 3.12

$$a_{12} = 0 \quad (3.12a)$$

$$a_{14} = 0 \quad (3.12b)$$

$$a_{15} = 0 \quad (3.12c)$$

$$a_{16} = 0 \quad (3.12d)$$

Step 4. Originally 16 unknown coefficients were associated with the assumed displacement polynomial of the element. By virtue of the four constraint equations, the unknowns associated with an element reduce to twelve.

3.4.2 Element geometry



Fig. 3.3 SFCFP - Element Geometry

The Geometry of Stress Field Consistent Four Node Quadrilateral Plate Bending Element (SFCFP) is given in fig.3.3. The element has four corner nodes. Each node has three degrees of freedom, namely $w, \partial w/\partial x, \partial w/\partial y$.

3.5 Generation of stiffness matrices and evaluation of nodal displacements

The stiffness matrix of each element can be developed by the conventional methods used in displacement based finite elements.

The stiffness matrix $[K] = \int_V [B]^T [D] [B] dV$ where $[D]$ contains the stress strain relations (moment – curvature relations in the case of plate bending element) and $[B]$ contains the strain displacement matrix (curvature - displacement matrix).

Displacement field $[u] = [x][P]^{-1}[d]$ where $[x]$ is the matrix containing polynomial terms and $[P]$ is the coefficient of shape function matrix including the constraint equation and $[d]$ is the nodal displacement vector.

Strain displacement matrix $[B]$ is defined as $[\partial][N]$ where $[N]$ is the shape function matrix.

$$[B] = [\partial][X][P]^{-1} \quad (3.13)$$

Using the above description expression for stiffness matrix can be rewritten as

$$[K] = \int_V [P]^{-1T} [X]^T [\partial]^T [D] [\partial][X][P]^{-1} dV \quad (3.14)$$

The elemental stiffness matrices are assembled to get the global stiffness matrix. The required nodal displacement vector is calculated by using the standard elimination process.

3.6 Software development for the implementation of field equilibrium finite elements

3.6.1 General

The flow chart of the software is shown in fig.3.4. Based on the same flow chart, three different computer programs based on modular concepts have been developed in Fortran 77, for implementing plane stress, three dimensional and plate bending field equilibrium finite elements. Details of each of these are described subsequently.

3.6.2 Plane stress elements

The input data file **plst1.dat** contains the detailed problem description including the number of nodes, element connectivity, loading details, boundary conditions, coordinates of points at which the stresses are to be calculated. The supporting data file **plstfu1.dat** contains details of displacement functions, their derivatives and Gauss quadrature data for numerical integration. The output (result) data file **plst1.out** contains detailed problem description and numerical results such as displacement at each nodal degree of freedom, stresses computed at the points specified in the input data file. Sequence of operations is listed below.

- (a). The main program accepts the detailed problem description from the input data file and the displacement function details from the supporting data file.
- (b). Then the displacement degrees of freedom are numbered globally and stored as **NDF()**
- (c). Load vector is generated based on the loading details provided in the input data file.

- (d). Based on the nodal connectivity, global degrees of freedom $NDF()$ is transferred to $MB()$ applicable to each individual element.

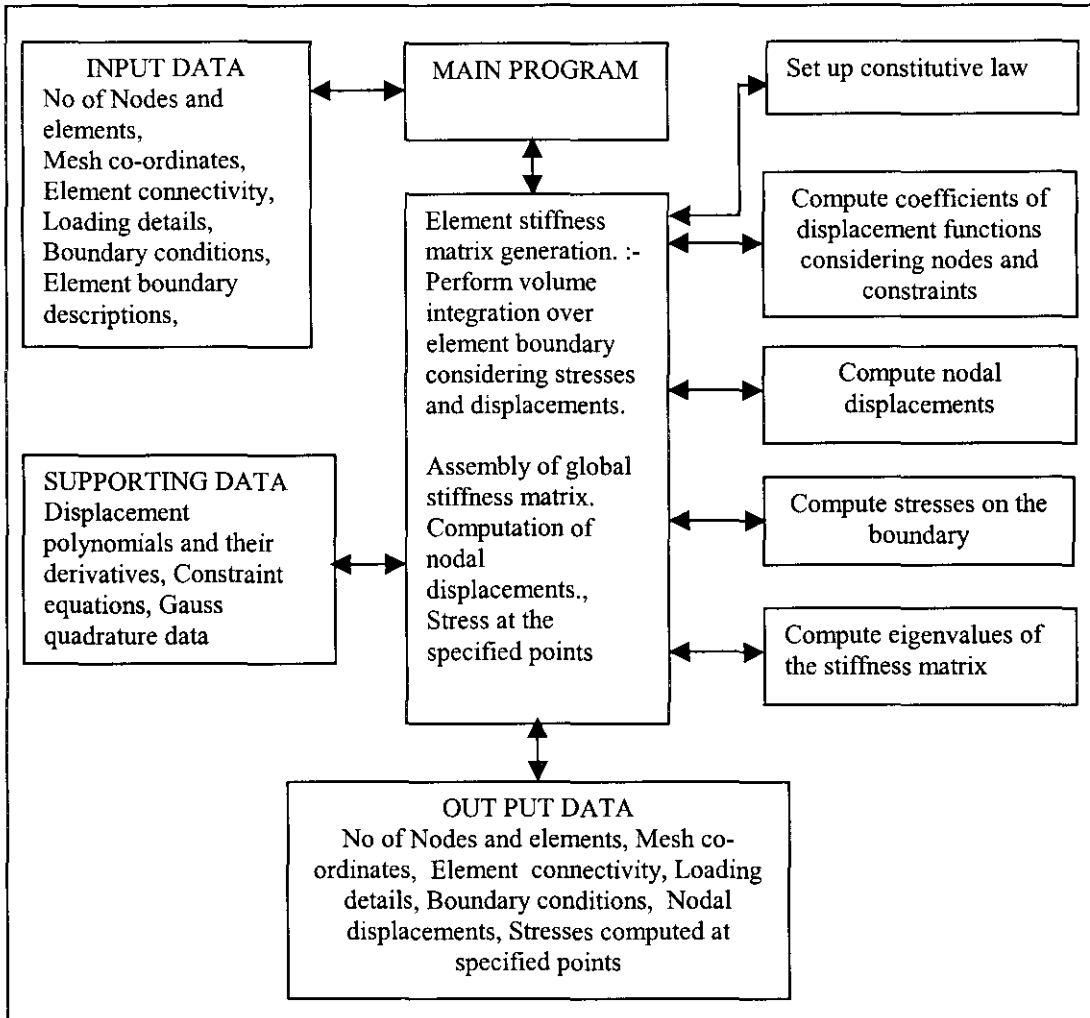


Fig. 3.4 Schematic flow diagram of the Computer Program

- (e). Global and local co-ordinates of each node are generated.
- (f). Value of each local co-ordinate is substituted in the corresponding terms in displacement polynomial to obtain the matrix $COSHF$. The remaining rows of $COSHF$ are filled with corresponding terms in the constraint equations.
- (g). The points of integration $XP()$, $YP()$ and weights of integration are generated. These points are substituted in the corresponding terms in derivative of displacement function to get $[EPS]$

- (h). $[\text{COSH}]^{-1} [\text{TRNSFR}] = [\text{CFTR}]$
- (i). $[\text{EPS}] [\text{CFTR}] = [\text{EPSL}]$
- (j). $[\text{DSTF}] = [\text{EPSL}]^T [\text{SSR}] [\text{EPSL}]$
- (k). $[\text{DSTF}]$ when multiplied with corresponding weights of integration and on summation gives $[\text{K}]$
- (l). Elemental stiffness matrices are assembled to get global stiffness matrices.
- (m). The required displacement vector is calculated by using standard elimination process.
- (n). A subroutine 'EIGCHK' is also provided for calculating the eigenvalues of the stiffness matrix and there by checking whether the rigid body modes are satisfied.
- (o). In order to calculate the stress at the specified grid points, the element in which the given grid point exists is first identified. Then the nodal displacement vector for that particular element $\{\text{EGDE}\}$ is collected.

$$[\text{TRN}]\{\text{EGDE}\} = \{\text{ELDEF}\}$$

$$[\text{COSH}]^{-1} \{\text{ELDEF}\} = [\text{UCOF}]$$

Then the grid points are located in local co-ordinate system and substituted in the derivatives of displacement function to get $[\text{EPS}]$

$$[\text{EPS}] [\text{UCOF}] = [\text{EPSL}]$$

$$[\text{SSR}] [\text{EPSL}] = [\text{STRESS}]$$

3.6.3 Three dimensional elements

The input data file **plst3.dat** contains the detailed problem description including the number of nodes, element connectivity, loading details, boundary conditions, co-ordinates of points at which the stresses are to be calculated. The supporting data file **plstfu3.dat** contains details of displacement functions, their derivatives and Gauss quadrature data for numerical integration. The output (result) data file **plst3.out** contains detailed problem description and numerical results such as displacement at

each nodal degree of freedom, stresses computed at the points specified in the input data file. The sequence of operations is listed below.

- (a). The main program accepts the detailed problem description from the input data file and the displacement function details from the supporting data file.
- (b). Then the displacement degrees of freedom are numbered globally and stored as **NDF()**
- (c). Load vector is generated based on the loading details provided in the input data file.
- (d). Based on the nodal connectivity, global degrees of freedom **NDF()** is transferred to **MB()** applicable to each individual element.
- (e). Global and local co-ordinates of each node are generated.
- (f). Value of each local co-ordinate is substituted in the corresponding terms in displacement polynomial to obtain the matrix **COSHF**. The remaining rows of **COSHF** are filled with corresponding terms in the constraint equations.
- (g). The points of integration **XP()**, **YP()**, **ZP()** and weights of integration are generated. These points are substituted in the corresponding terms in derivative of displacement function to get **[EPS]**
- (h). $[\text{COSHF}]^{-1} [\text{TRANSFR}] = [\text{CFTR}]$
- (i). $[\text{EPS}] [\text{CFTR}] = [\text{EPSL}]$
- (j). $[\text{DSTF}] = [\text{EPSL}]^T [\text{SSR}] [\text{EPSL}]$
- (k). **[DSTF]** when multiplied with corresponding weights of integration and on summation gives **[K]**
- (l). Elemental stiffness matrices are assembled to get global stiffness matrices.
- (m). The required displacement vector is calculated by using standard elimination process.

- (n). A subroutine 'EIGCHK' is also provided in the program for calculating the eigenvalues of the stiffness matrix and there by checking whether the rigid body modes are satisfied.
- (o). In order to calculate the stress at the specified grid points, the element in which the given grid point exists is first identified. Then the nodal displacement vector for that particular element {EGDE} is collected.

$$[\text{TRN}]\{\text{EGDE}\} = \{\text{ELDEF}\}$$

$$[\text{COSH}]^{-1} \{\text{ELDEF}\} = [\text{UCOF}]$$

Then the grid points are located in local co-ordinate system and substituted in the derivatives of displacement function to get [EPS]

$$[\text{EPS}] [\text{UCOF}] = [\text{EPSL}]$$

$$[\text{SSR}] [\text{EPSL}] = [\text{STRESS}]$$

3.6.4 Plate bending elements

The input data file **plbe.dat** contains the detailed problem description including the number of nodes, element connectivity, loading details, boundary conditions etc. The supporting data file **plbefu.dat** contains the details of displacement functions, their derivatives and Gauss quadrature data for numerical integration. The output (result) data file **plbe.out** contains detailed problem description and the numerical results such as displacements at each nodal degree of freedom. The sequence of operations is listed below.

- (a). The main program accepts the detailed problem description from the input data file and the displacement function details from the supporting data file.
- (b). Then the displacement degrees of freedom are numbered globally and stored as **NDF()**

- (c). Load vector is generated based on the loading details provided in the input data file.
- (d). Based on the nodal connectivity, Global degrees of freedom $\mathbf{NDF}(\)$ is transferred to $\mathbf{MB}(\)$ applicable to each individual element.
- (e). Local and global co-ordinates of each node are generated.
- (f). Value of each local co-ordinate is substituted in the corresponding terms in the displacement polynomial to obtain the matrix \mathbf{COSHf} . The remaining rows of the \mathbf{COSHf} are filled with corresponding terms in the constraints equation.
- (g). The points of integration $\mathbf{XP}(\)$, $\mathbf{YP}(\)$ and the weights of integration are generated. These points are substituted in the corresponding terms in the derivative of displacement function to get $[\mathbf{EPS}]$
- (h). The points of integration $\mathbf{XP}(\)$, $\mathbf{YP}(\)$ and weights of integration are generated. These points are substituted in the corresponding terms in derivative of displacement function to get $[\mathbf{EPS}]$
- (i). $[\mathbf{COSHf}]^{-1} [\mathbf{TRNSFR}] = [\mathbf{CFTR}]$
- (j). $[\mathbf{EPS}] [\mathbf{CFTR}] = [\mathbf{EPSL}]$
- (k). $[\mathbf{DSTF}] = [\mathbf{EPSL}]^T [\mathbf{SSR}] [\mathbf{EPSL}]$
- (l). $[\mathbf{DSTF}]$ when multiplied with corresponding weights of integration and on summation gives $[\mathbf{K}]$
- (m). Elemental stiffness matrices are assembled to get global stiffness matrices.
- (n). The required displacement vector is calculated by using standard elimination process.
- (o). A subroutine 'EIGCHK' is also provided in the program for calculating the eigenvalues of the stiffness matrix and there by checking whether the rigid body modes are satisfied.

3.7 Numerical investigations on performance of the elements

The numerical investigations on performance of the elements have been carried out by testing it in standard test problems. The results are compared with exact solutions and the results obtained with other established displacement based finite elements in the next three chapters.

CHAPTER 4

PERFORMANCE COMPARISON OF PLANE STRESS ELEMENT (SFCNQ)

4.1 General

Numerical investigations on the performance of Stress Field Consistent Nine Node Quadrilateral element -SFCNQ have been carried out through standard test problems for validation purpose. Comparisons involving theoretical closed form solutions as well as solutions from the existing finite elements have also been made.

Eigenvalue test is performed on the element in order to conform the presence of adequate rigid body modes. It has been discussed in section 2.2.1 that the performance of two dimensional elements with translational degrees of freedom, when used to model in-plane bending found to be lacking accuracy. Hence, test problems involving in-plane bending are also carried out. Application of this element to stress concentration studies are considered next. Patch test has also been performed on two cases. These test details are described under subsequent subheadings.

4.2 Eigenvalue test

The eigenvalue test is used to evaluate the element quality (Dow *et al.* 1984). It is used to detect zero energy deformation modes and rigid body motion capability of the element. An unrestrained element is considered for the eigenvalue test, so that $[k]$ is complete element stiffness matrix.

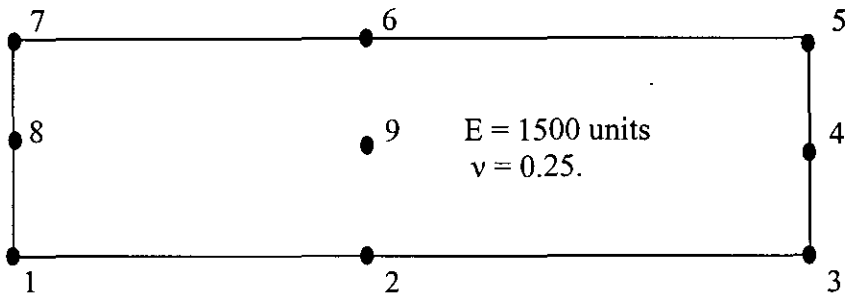


Fig.4.1 Eigenvalue test model using single element

A beam of size 10 x 1 x 1 is modelled with a single element as shown in fig. 4.1. Material properties are considered as $E = 1500$ units and $\nu = 0.25$. The element stiffness matrix and global stiffness matrix are same for this problem. The element has 2 dof per node and 18 dof in total. Stiffness matrix and eigenvalues of unrestricted element are calculated and are given in table 4.1.

Table 4.1 Eigenvalues computed from stiffness matrix of SFCNQ

Sl No.	Eigenvalues	Sl No.	Eigenvalues	Sl No.	Eigenvalues
1	0.58899E+07	7	0.24183E+04	13	0.26866E+03
2	0.21037E+06	8	0.13173E+04	14	0.25667E+03
3	0.45208E+04	9	0.10968E+04	15	0.23489E+03
4	0.32518E+04	10	0.10733E+04	16	0.35759E-10
5	0.25572E+04	11	0.86798E+03	17	-0.58384E-12
6	0.24183E+04	12	0.71816E+03	18	-0.79428E-10

All the 18 eigenvalues are real and positive and among them, three zeros or near zero values are obtained, showing that the element is exhibiting three rigid body modes.

When the element is reoriented in global co-ordinates by changing the node

numbering sequence, the eigenvalues do not change, indicating the geometric invariance of the element. Hence, it is inferred that the stiffness matrix is real, positive semi definite and the element is geometrically isotropic.

4.3 Problems with in-plane bending

An attempt has been made to examine various aspects of modelling the bending behaviour by the element SFCNQ. Performance of elements with various aspect ratios and distorted geometry are examined. The test problems considered are MacNeal- Harder thin cantilever beam and deep cantilever beam.

4.3.1 MacNeal – Harder thin cantilever beam

The thin cantilever problem is a standard test problem for finite elements (MacNeal and Harder 1985). This test is simple and can be applied to beam, plate and solid elements. Moreover, all the element deformation modes can be evoked by applying suitable loads on the free end of the cantilever. This test will bring out the susceptibility of the element to shear and distortional locking.

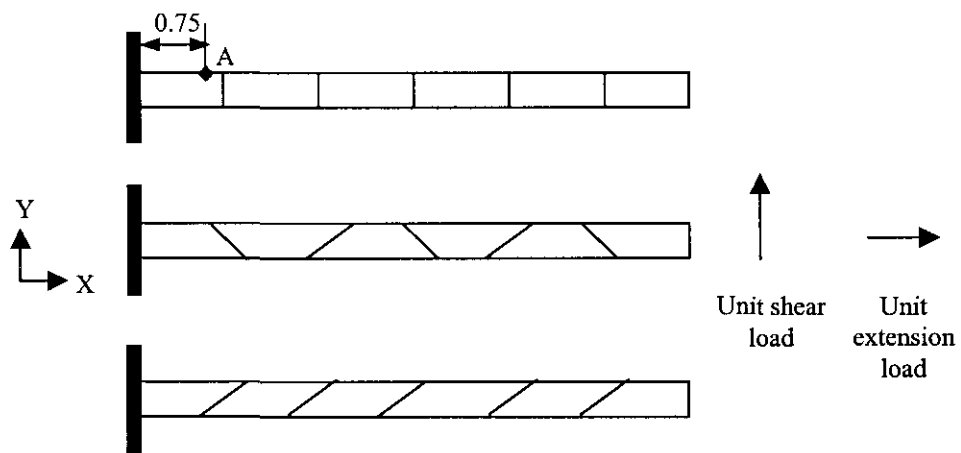


Fig. 4.2 MacNeal and Harder thin Cantilever beam

(a) Regular. (b) Trapezoidal (c) Parallelogram elements.
 Length – 6.0, width – 0.2, depth – 0.1, $E = 10^7$, $\nu = 0.3$, mesh – 6 x 1

A cantilever beam with a length, depth and width of 6.0, 0.2 and 0.1 units are idealised with three types of element geometries namely regular, trapezoidal and parallelogram elements as shown in fig. 4.2. A unit in-plane load is applied on the free end of the beam. Nodal displacement and stress at point A (shown in fig.4.2) are evaluated. Normalised tip displacements and stresses are tabulated in table 4.2 and 4.3 respectively. The element with regular geometry underestimates the displacement by 2.6% and overestimates the stress by 5.4 %. The element with trapezoidal geometry underestimates the displacement by 1.9% and overestimates the stress by 1%. The element with parallel geometry under-estimates the displacement by 2.2% and overestimates the stress by 1.6%.

Table 4.2 Normalised Tip displacements from MacNeal-Harder thin cantilever beam test under shear load

SI No.	Element	Normalised Tip Displacement		
		Regular	Trapezoidal	Parallel
1	HEXA 20*	0.970	0.886	0.967
2	HEXA20R*	0.984	0.964	0.994
3	SFCNQ	0.974	0.981	0.978

* Source :- MacNeal and Harder 1985

Table 4.3 Normalised Stress σ_x from MacNeal-Harder thin cantilever beam test under shear load

SI No.	Element	Normalised Stress		
		Regular	Trapezoidal	Parallel
1	ANSYS	0.972	0.977	0.976
2	SFCNQ	1.054	1.010	1.016

Table 4.4 Normalised Tip displacements from MacNeal-Harder thin cantilever beam test under extension load

SI No.	Element	Normalised Tip Displacement		
		Regular	Trapezoidal	Parallel
1	HEXA 20	0.994	0.994	0.994
2	HEXA20R	0.999	0.999	0.999
3	SFCNQ	1.000	1.000	1.000

Table 4.5 Normalised Stress σ_x from MacNeal-Harder thin cantilever beam test under extension load

SI No.	Element	Normalised Stress		
		Regular	Trapezoidal	Parallel
1	ANSYS	1.000	1.160	1.170
2	SFCNQ	1.000	1.030	1.010

In the extension test a unit extension load is applied at the free end the cantilever. Nodal displacement and stress at specified location (shown in fig.4.2) are evaluated and tabulated in table 4.4 and 4.5 respectively. The stresses and displacements predicted by the SFCNQ are in general agreement with the theoretical values. Irrespective of the geometry of the element, it predicts the tip displacements exactly. However, a nominal error of 3% and 1% are observed in stress predictions by elements with trapezoidal and parallel geometry.

4.3.2 Deep cantilever beam with rectangular elements

In this test, a deep beam of length 10.0, width 2.0 and depth 1.0 is discretised with single layer of elements along the span of the beam as shown in fig.4.3. A single layer of elements is a stringent test as it is the usual practice to increase the depth wise layers to reduce the parasitic shear effect. Two load cases are considered in this test viz., unit moment (load case a) and unit extension load (load case b). Normalised tip-

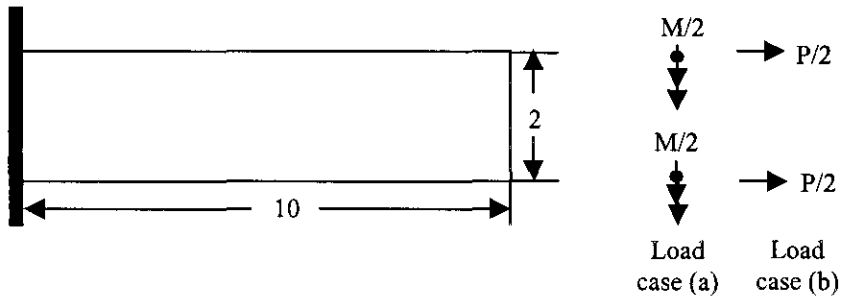


Fig. 4.3 Deep Cantilever modelled with rectangular elements. $E = 1500$. units, $\nu = 0.25$

displacements in thin beam ($l/h = 100$) and thick beam ($l/h = 5$) situations are evaluated and shown in table 4.6 and 4.7 respectively. The beam is modelled with single element, two elements and three elements mesh. It has been found that in the case of unit moment load, the error in predicted tip displacements with single element, two element and four element situations are 1.7 %, 1.0 % and 0.87% respectively. In the case of extension load, the element is able to predict exact displacement and stress even in single element situation.

Table 4.6 Normalised tip displacements for thin deep cantilever beam. ($l/h = 100$)

Sl. No.	Element	Normalised Tip Displacements					
		Load case a.			Load case b.		
		Single element	Two elements	Four elements	Single element	Two elements	Four elements
1	Dvorkin and Bathe	100	100	100	75	-	98.4
2	HMPL5	100	100	100	94	-	100
3	SFCNQ	101.7	101.0	100.87	99.68	100.1	100.1

Results are also compared with that obtained with two well performing elements HMPL5 (Saleeb and Chang 1987) and a nine node hybrid stress element (Dvorkin and Bathe 1984). It is found that the performance of these elements is slightly better than -

Table 4.7 Normalised tip displacements for thick deep cantilever beam. ($l/h = 5$)

Sl. No.	Element	Normalised Tip Displacements					
		Load case a.			Load case b.		
		Single element	Two elements	Four elements	Single element	Two elements	Four elements
1	Dvorkin and Bathe	100	100	100	75	-	98.4
2	HMPL5	100	100	100	94	-	100
3	SFCNQ	101.9	101	100.85	100.	100.	100.

SFCNQ in load case a. However, the results obtained with SFCNQ also converge to the exact value when the element mesh increases to 4×1 . In the case of extension load (load case b) SFCNQ out performed the other two elements. It gives near exact value, even in single element situation.

4.3.3 Distortion test

Influence of geometric distortion of the element on its performance is investigated. Performance of most of the elements is affected when they are distorted or used as quadrilaterals rather than rectangles. In this test, a deep beam is idealised with various element geometries for testing the effect of geometric distortion of the element in its performance in deep beam situations (Dvorkin and Bathe 1984).

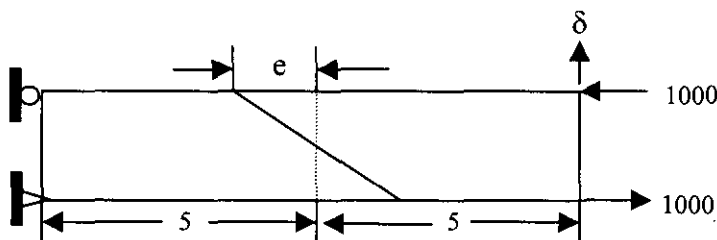


Fig. 4.4 Two element distortion sensitivity test.

In the two-element distortion sensitivity test, a deep beam of size 10 x 2 x 1 is idealised with two elements of different geometries. The problem is described in fig.4.4. A couple of 2000 units is applied at the free end of the beam.

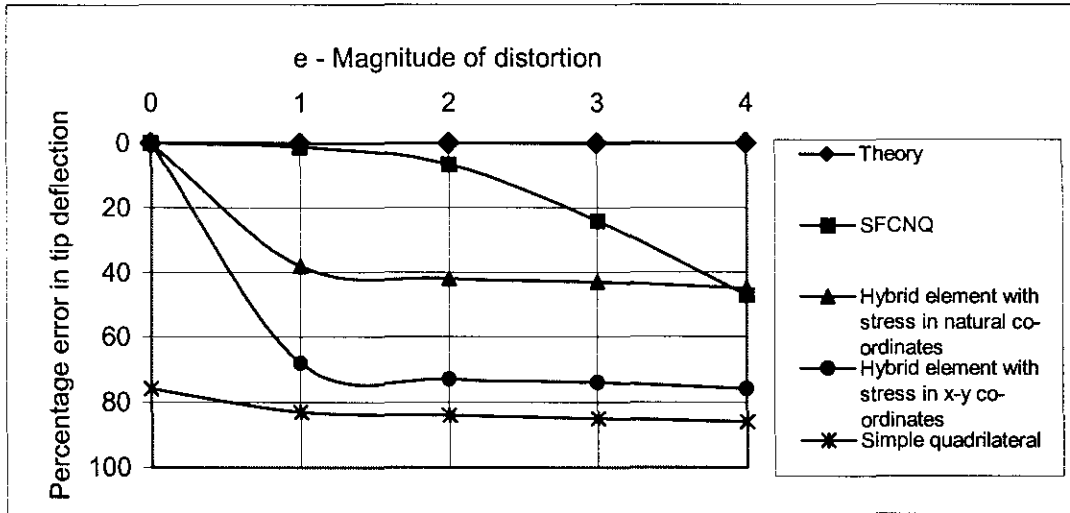


Fig. 4.5 Distortion sensitivity test- Percentage error in tip displacement Vs magnitude of geometric distortion

The tip deflection is evaluated with distorted element geometries. The geometric distortion of the element is increased by successively varying the value of 'e' from zero to four as explained in fig.4.4. The percentage error in tip deflection δ is plotted against the geometric distortion 'e' of the element in fig.4.5. The percentage errors in predicted tip deflection increases from near zero value for undistorted geometry to 47% for an extreme geometric distortion 'e' of 4. The performance of the element is also compared with theory and that of existing elements like hybrid element with stresses in ξ - η co-ordinates, hybrid element with stresses in x-y co-ordinates and simple quadrilateral (Source :- Cook and Jaafar 1969), in the same figure. It is inferred from the results that the element is capable of predicting almost exact results for geometrical distortions, which are within the general acceptable range.

4.4 Stress concentration problems

Test problems considered are infinite plate with circular discontinuity at the centre subjected to uniform tension and circular disc with concentrated edge load.

4.4.1 Infinite plate with circular cut out at the centre

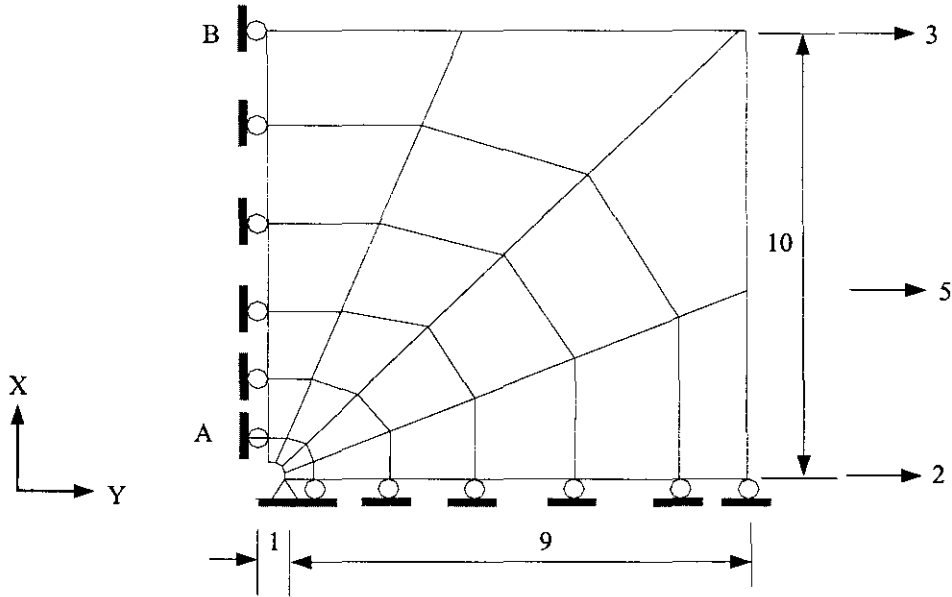


Fig. 4.6 Infinite plate with a circular discontinuity at the centre
 $E = 1500$, $t = 1.0$, $\nu = 0.25$

An infinite plate with a circular hole at the centre, under uniform tension in one direction (Timoshenko and Goodier 1951) is modelled with a finite element mesh as shown in fig.4.6. The diameter of the hole is $1/10$ of the length of the plate. Only one quarter of the plate is modelled, taking advantage of the geometric and load symmetry. The distribution of the σ_y along the line AB is compared with QUAD 4 (a bilinear element) in fig. 4.7. It has been found that SFCNQ captures a stress concentration factor of 2.9 (exact value is 3.0) even with a course mesh. The general trend of variation stress in the direction of the load is also well represented.

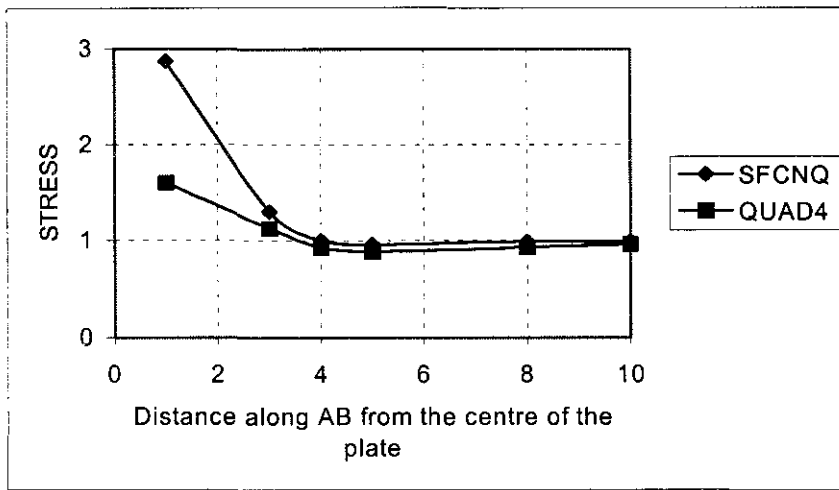


Fig. 4.7 Stress computed along the edge AB of an infinite plate with a discontinuity at the centre.

4.4.2 Circular disc with concentrated edge load

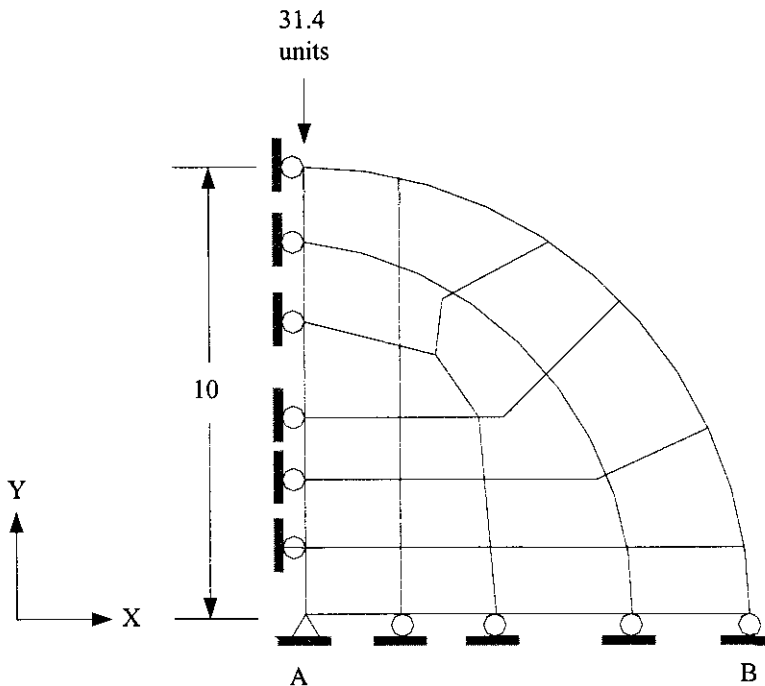


Fig. 4.8 Circular disc with concentrated edge load
 $E = 1500$ units, $\nu = 0.25$, thickness = 1.0 units

A circular disc with concentrated vertical load at its top is considered in this problem. The problem is described in fig. 4.8. Taking advantage of the geometric and load symmetries, only one quadrant of the disc is modelled. The stress values (σ_y) along

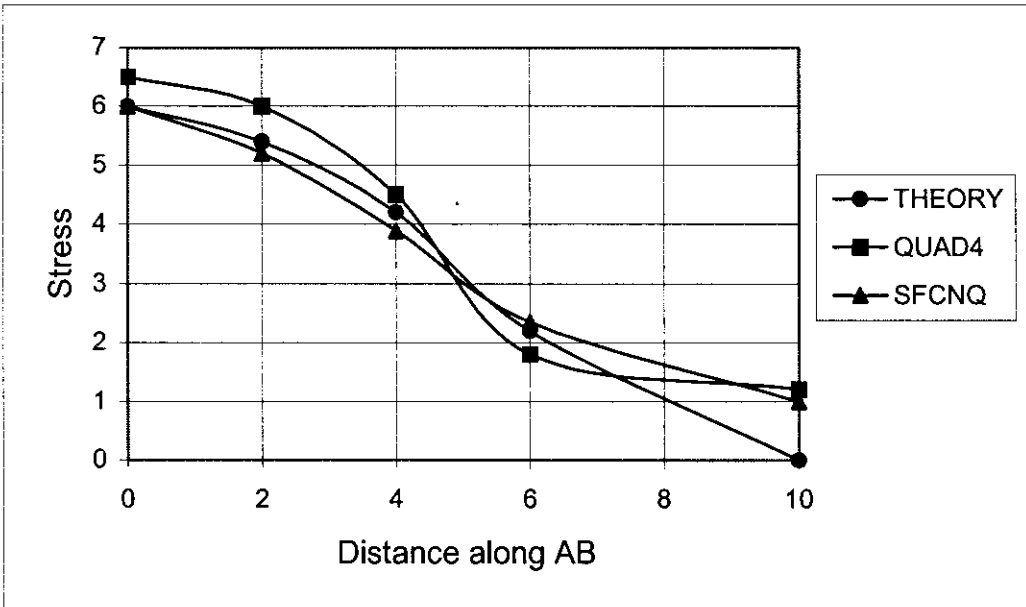


Fig. 4.9 Stress distribution along the diameter of the circular disc with concentrated edge load

diameter of the disc or on the base of the quadrant are evaluated. The stress distribution along the diameter of the disc is compared with the theoretical values and solution obtained with QUAD4 (a basic bilinear isoparametric element) in fig.4.9. It can be seen that SFCNQ represents the peak stress at the centre of the disc and the general trend of stress distribution is also well represented.

4.5 Patch tests

The patch test was originally proposed by Irons *et al.*(1965). This test is used to check the validity of the element formulation and its implementation. The patch test serves as a necessary and sufficient condition for correct convergence of finite element formulation. The patch test consists of applying constant stress or strain to an arbitrary patch of elements. If the element predicts constant stress at all points within, then it is considered to have passed the patch test. If the element predicts the expected state of constant stress, as the mesh is repeatedly subdivided, then it is said to have passed the

weak patch test. If the element passes the weak patch test then also, the correct convergence of finite element formulation is assured.

4.5.1 Constant strain Patch test

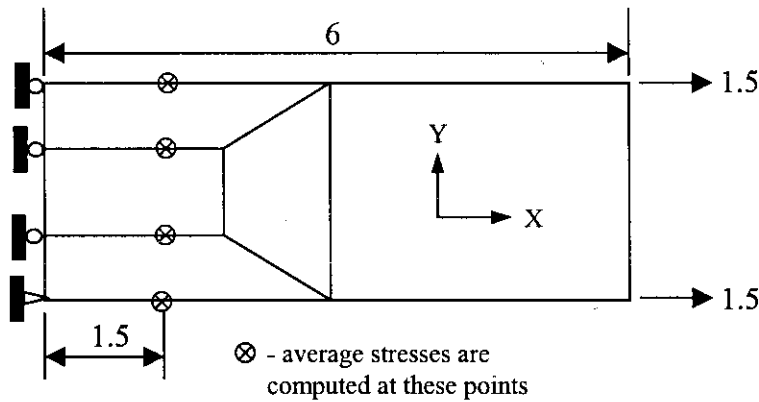


Fig. 4.10 Element mesh for constant strain patch test
 $E = 1.0$, $\nu = 0.25$, size $6 \times 3 \times 1$

A patch of elements subjected to a load, simulating constant stress and strain condition (Irons *et al.* 1965) is considered. The problem is described in fig.4.10. The tip displacements and stresses at the specified points (shown in fig.4.10) are evaluated and shown in table 4.8.

Table 4.8 Tip displacements and average stresses computed from constant strain patch test

Sl. No.	Element	Tip Displacements		Average Stresses σ_{xx}	
		Mesh : 5 elements	Mesh : 20 elements	Mesh : 5 elements	Mesh : 20 elements
1	ANSYS	6.0	6.0	1.0	1.0
2	THEORY	6.0	6.0	1.0	1.0
3	SFCNQ	7.5	6.0	1.03	1.0

It has been found that for a five element mesh the solutions obtained with SFCNQ is not exactly matching with theory. The percentage errors for the computed values of tip displacements and stresses are 25 and 3.71 respectively. When the problem is modelled with a refined twenty-element mesh, the displacements and stresses do converge to the exact value. Here a twenty-element mesh is obtained by joining the mid points of edges of each element.

4.5.2 Weak patch test

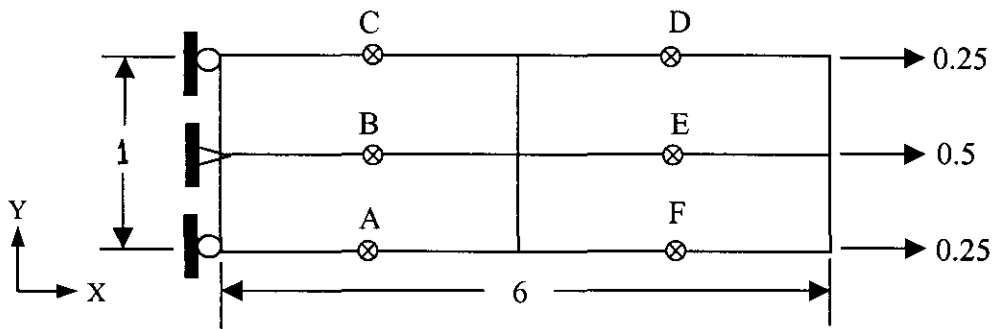


Figure 4.11 Element mesh for weak patch test

In this test a beam of size $6 \times 1 \times 1$ is idealised with four undistorted elements as shown in fig.4.11. The material properties are taken as $E = 1.0$ and $\nu = .25$. A unit extension load is applied on the free end of the beam and the stresses are evaluated at points specified in the figure. The results are tabulated and compared with theoretical values in Table 4.9. It has been found that the stresses computed are constant and the maximum percentage deviation from the theoretical value is of the order of 2 percentage.

Table 4.9 Average stresses (σ_{xx}) obtained from Weak Patch test.

Sl No.	Point at which average stresses are computed.	Stress σ_{xx}	
		SFCNQ	Theory
1	A	1.015	1.0
2	B	1.003	1.0
3	C	1.005	1.0
4	D	1.023	1.0
5	E	0.989	1.0
6	F	0.990	1.0

4.6 Remarks

The new element SFCNQ has been tested in different standard test problems. It performs well in all the situations considered, except in the patch test. SFCNQ is a nonconforming element, as the displacements of points along the edges of the element do not fully depend on the nodes lying in that edge. Hence, SFCNQ pass the patch test only in an average sense. However, the element passes the weak patch test and gives consistently good results in all the other test problems considered.

CHAPTER 5

PERFORMANCE COMPARISON OF THREE DIMENSIONAL ELEMENT (SFCSS)

5.1 General

Numerical investigations on the performance of Stress Field Consistent Sixteen Node Solid element - SFCSS have been carried out through standard test problems for validation purpose. Comparisons involving theoretical closed form solutions as well as solutions from the existing finite elements have also been made.

The following numerical tests have been carried out using the element SFCSS.

- eigenvalue test.
- aspect ratio sensitivity test.
- beam tests.
- patch tests.
- Boussinesq problem
- curved shell test.

The performance of the element SFCSS is compared with the performance of other elements reported in literature and also with that obtained from STF - 45 element of a commercially available finite element software package (ANSYS version 5.3, 2000). Wherever exact numbers have not been reported in the literature, the values have been read off from relevant graphs and figures. These test details are described under subsequent subheadings.

5.2 Eigenvalue test

The eigenvalue test is used to evaluate the element quality (Dow *et al.* 1984) It is used to detect zero energy deformation modes and rigid body motion capability of the element. An unrestrained element is considered for the eigenvalue test, so that $[k]$ is complete element stiffness matrix.

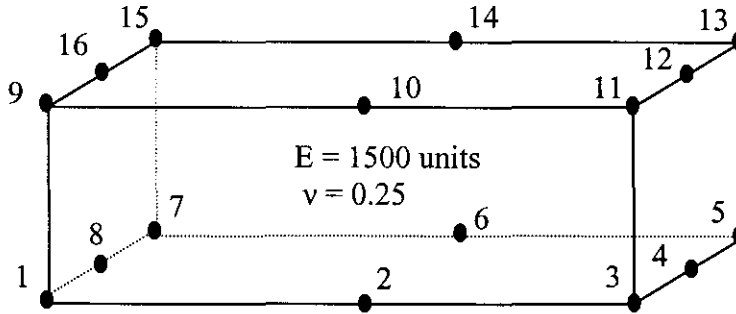


Fig 5.1 Eigenvalue test model using single element

A beam of size $10 \times 1 \times 1$ is modelled with a single element as shown in fig. 5.1. Material properties are considered as $E = 1500$ units and $\nu = 0.25$. The element stiffness matrix and global stiffness matrix are same for this problem. The element has 3 dof per node and 48 dof in total. Stiffness matrix and Eigenvalues of unrestricted element are calculated using the computer code Plst3.for and are given in table 5.1. All the 48 eigenvalues are real and positive and among them, six zeros or near zero values are obtained, showing that the element is exhibiting six rigid body modes. When the element is reoriented in global co-ordinates by changing the node numbering sequence, the eigenvalues do not change, indicating the geometric invariance of the element. Hence, it is inferred that the stiffness matrix is real, positive semi definite and the element is geometrically isotropic.

627.04
JAN 31

Table 5.1 Eigenvalues computed from stiffness matrix of SFCSS

SINo	Eigenvalue	SINo	Eigenvalue	SINo	Eigenvalue	SINo	Eigenvalue
1	.61772E+10	13	.25786E+01	25	.48534E+00	37	.12431E+00
2	.31274E+10	14	.20727E+01	26	.40445E+00	38	.10842E+00
3	.26585E+09	15	.15265E+01	27	.39019E+00	39	.10841E+00
4	.88615E+08	16	.14488E+01	28	.38364E+00	40	.10837E+00
5	.41902E+08	17	.14487E+01	29	.33027E+00	41	.10360E+00
6	.41890E+08	18	.11264E+01	30	.33018E+00	42	.85470E+00
7	.29776E+02	19	.95454E+00	31	.30865E+00	43	.61711E-07
8	.29775E+02	20	.95439E+00	32	.23059E+00	44	.15254E-07
9	.36989E+01	21	.74781E+00	33	.19216E+00	45	-.16121E-09
10	.35707E+01	22	.49816E+00	34	.19211E+00	46	-.28625E-07
11	.35705E+01	23	.49807E+00	35	.15565E+00	47	-.77416E-07
12	.32549E+01	24	.48543E+00	36	.12708E+00	48	-.13584E-06

5.3 Aspect ratio sensitivity test

Robinson (1986) proposed the single element test for aspect ratio sensitivity. This is a simple test in which the elements of various aspect ratios are subjected to a bending load under cantilevered conditions as shown in the fig. 5.2 Tip deflections calculated using equations based on Euler- Bernoulli beam theory and two other finite element analysis results are tabulated together with the results of the present study in table 5.2. Solutions obtained with the element SFCSS nearly matches with those predicted by Euler - Bernoulli beam theory. The element with an aspect ratio of 1 is able to predict

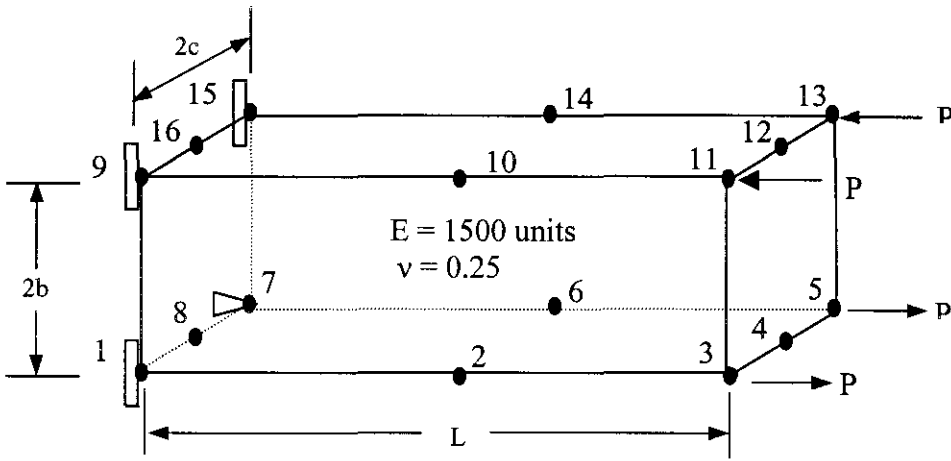


Fig . 5.2 Aspect ratio sensitivity test

$$E = 207 \times 10^9, b = c = 0.06, \nu = 0.25, P = 6900 \text{ units}$$

Table 5.2 Single element aspect ratio sensitivity test

Aspect ratio.	TIP DEFLECTION $\times 10^{+6}$			
	THEORY*	CSA NASTRAN*	ASKA*	SFCSS
1	3.33	3.125	3.115	3.23
2	13.33	12.50	12.50	12.78
4	53.33	50.00	49.75	50.00
8	213.33	200.00	161.20	198.60

* Source : Chandra and Prathap (1992)

exact solution and the percentage deviation from the theoretical tip displacement is increased to 7.5 when analysed with an element of aspect ratio eight.

5.4 Beam Tests

Beam tests are conducted in slender beam and deep beam situations.

5.4.1 Slender beam

The problem suggested by MacNeal and Harder (1985) is considered in this test. The cantilever beam with a length, width and depth of 6.0, 0.2

and 0.1 units is idealised with three types of element geometries namely regular, trapezoidal and parallelogram elements as shown in the figures 5.3a, 5.3b and 5.3c respectively. Two load cases were considered in this test. viz., shear load and extension load.

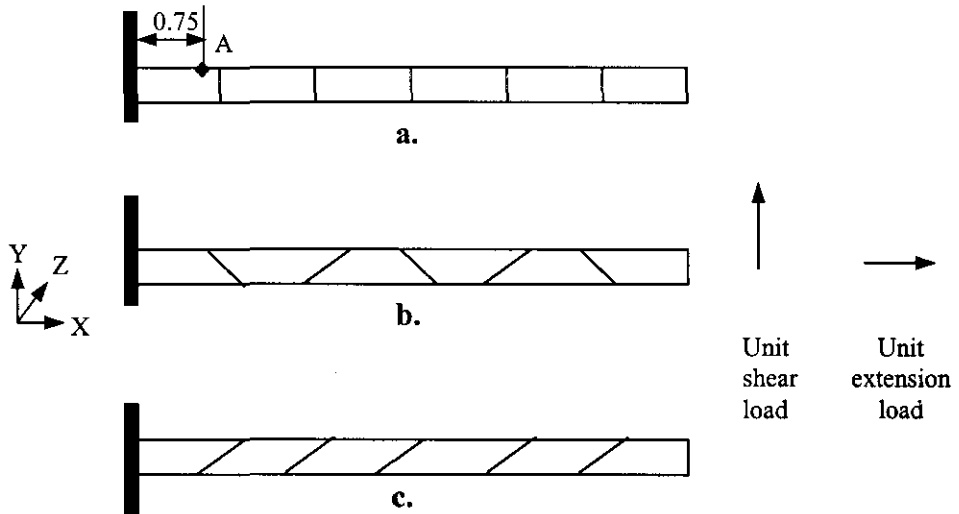


Fig. 5.3 MacNeal - Harder thin Cantilever beam

(a) Regular. (b) Trapezoidal (c) Parallelogram elements.

Length – 6.0, width – 0.2, depth – 0.1, $E = 10^7$, $\nu = 0.3$, mesh – 6×1

Table 5.3 Normalised tip displacements of a slender beam under shear load

Sl No.	Element	Normalised tip displacement		
		Regular	Trapezoidal	Parallel
1	HEXA(8)*	0.981	0.690	0.801
2	HEXA20*	0.970	0.886	0.967
3	HEXA20R*	0.984	0.964	0.994
4	RGD ₂₀ **	0.984	0.981	0.981
5	PT18 β ***	0.981	0.046	0.625
6	SFCSS	0.989	0.976	0.976

* Source : MacNeal and Harder (1985), **Source : Chen and Cheung(1992)

*** Source : Sze and Ghali (1993)

Table 5.4 Normalised stresses(σ_{xx}) at the root of a slender beam under shear load

Sl. No	Element	Normalised stress		
		Regular	Trapezoidal	Parallel
1	ANSYS	0.972	0.977	0.976
2	SFCSS	0.997	0.993	0.998

A unit in-plane shear load is applied at the free end of the beam as shown in the fig.5.3. The tip displacements, normalized with respect to the theoretical values are compared with the solutions obtained with the other existing elements in table 5.3 and the comparison of the normalised stresses at the root of the beam is shown in table 5.4. The element is able to predict 97.6 percentage of the theoretical tip displacements and 99.3 percentage of the theoretical value in the case of stresses at the root of the beam even with distorted elements.

In the extension test a unit extension load is applied at the free end of the cantilever as shown in the fig. 5.3 (MacNeal and Harder 1985). Table 5.5 shows the comparison of normalised displacements at the tip and table 5.6 gives the comparison of normalised stresses at the root of the beam. The stresses and displacements predicted by the element SFCSS are in general agreement with the theory. The maximum percentage error is 1.1 in the case of tip displacements and 11 in the case of stresses computed at the roots of the slender beam. In the case of extension load, all the elements perform reasonably well. The element SFCSS performed consistently well in both the load cases irrespective of the element geometry considered.

Table 5.5 Tip displacements of a slender beam under extension load

Sl. No	Element	Normalised tip displacement		
		Regular	Trapezoidal	Parallel
1	HEXA(8)*	0.988	0.989	0.989
2	HEXA20*	0.994	0.994	0.994
3	HEXA20R*	0.999	0.999	0.999
4	SFCSS	0.989	1.011	1.007

* Source : MacNeal and Harder (1985)

Table 5.6 Normalised stresses(σ_{xx}) at the root of a slender beam under extension load

Sl. No.	Element	Normalised stress		
		Regular	Trapezoidal	Parallel
1	ANSYS	1.00	1.16	1.17
2	SFCSS	1.00	1.11	1.04

5.4.2 Deep beam

In this test, a deep beam is idealised with various element geometries for testing the effect of geometric distortion of the element in its performance in deep beam situations. Distortion test concern the problems, which were first, used by Cheung and Chen(1988). In two element distortion sensitivity test, a deep beam of size 10 x 2 x 2 is idealised with two elements with different geometries. The geometrical distortion of the element is increased by successively varying the value of 'e' from zero to four as explained in fig. 5.4. Two load cases (shear load and bending moment load) are considered in the test.

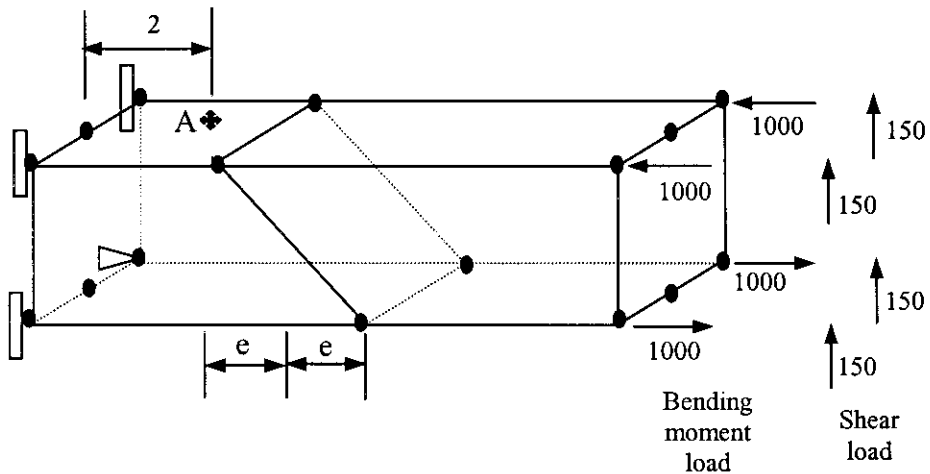


Fig . 5.4 Two element distortion sensitivity test using deep beam

$$E = 207 \times 10^9, \nu = 0.25, \text{ size - } 10 \times 2 \times 2 \text{ units}$$

The tip displacements and stresses are computed with successively increasing geometrical distortion of the element under shear load and are compared with that of theory and other existing elements in figures 5.5 and 5.6 respectively. The percentage errors in predicted tip deflections and stresses increase from near zero values for undistorted geometry to 70% for an extreme geometric distortion 'e' of 4.

The variation in the tip displacement and stresses with the increasing geometrical distortion of the element under bending moment load are computed and tabulated in figures 5.7 and 5.8 respectively. The percentage errors in predicted tip deflections and stresses increase from near zero values for undistorted geometry to 12% for an extreme geometric distortion 'e' of 4. From the above results it can be seen that the element SFCSS is capable of predicting almost exact results for geometric distortions, which are within the general acceptable range.

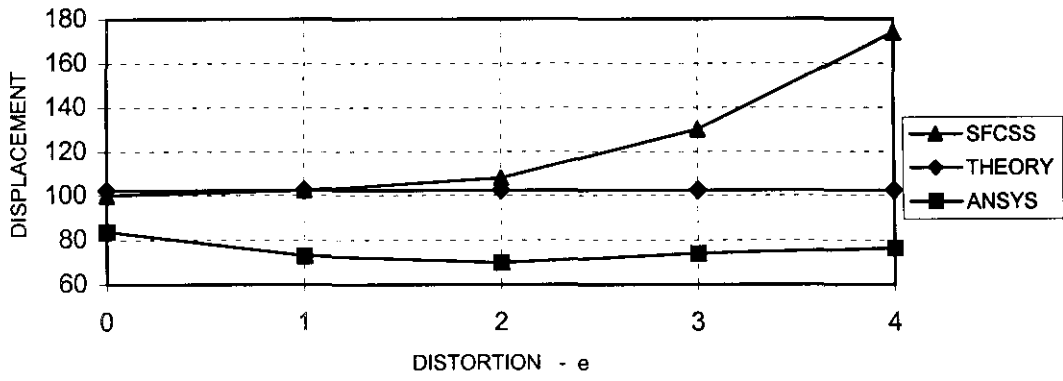


Fig. 5.5 Two element distortion sensitivity test for tip displacement (v) under shear load

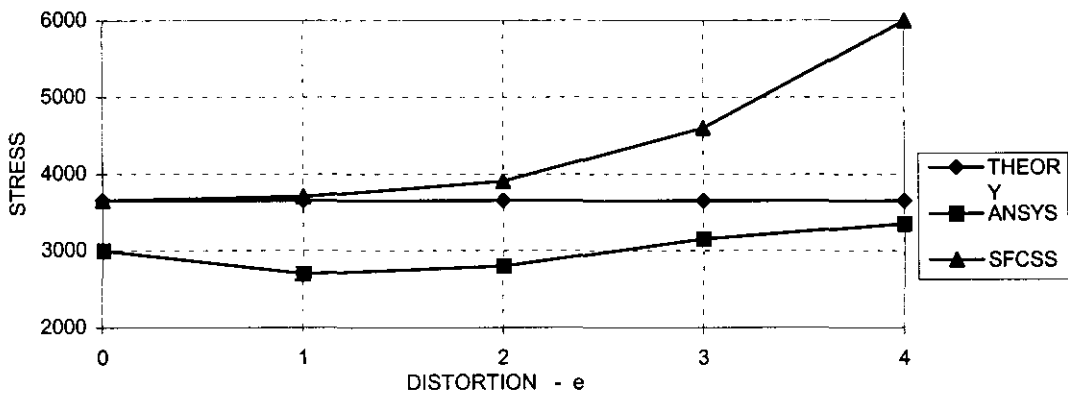


Fig. 5.6 Two element distortion sensitivity test for stress under shear load

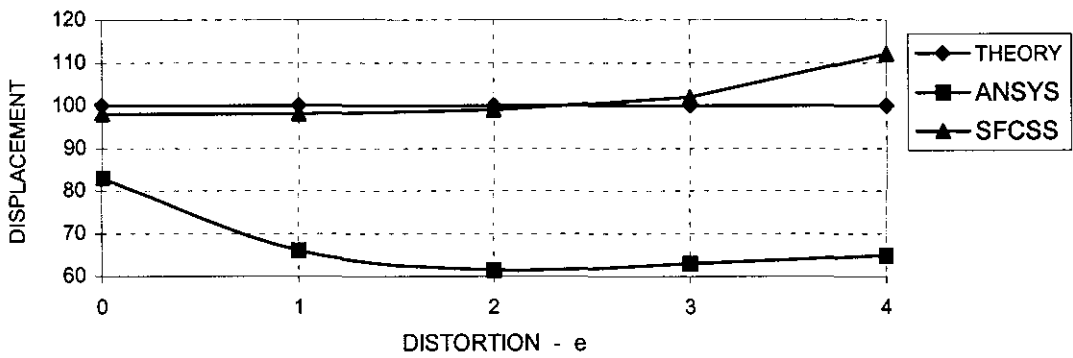


Fig. 5.7 Two element distortion sensitivity test for tip displacement (v) under bending load.

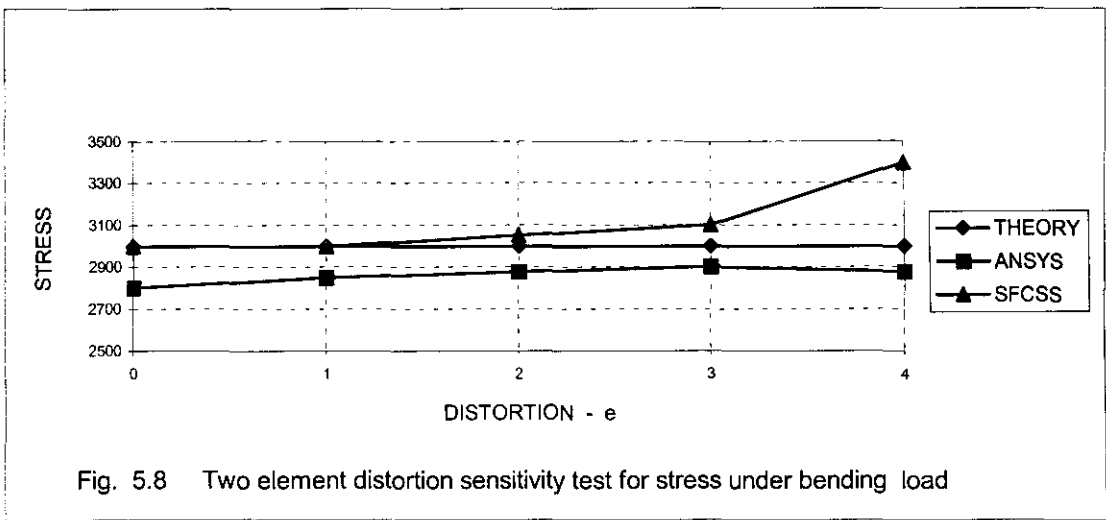


Fig. 5.8 Two element distortion sensitivity test for stress under bending load

5.5 Patch tests

Two types of patch tests are considered in this category namely, constant strain patch test and weak patch test.

5.5.1 Constant strain patch test

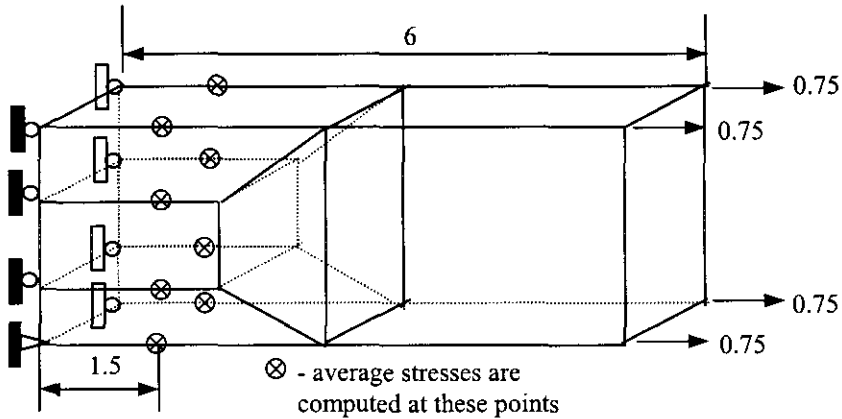


Fig. 5.9 Element mesh for constant strain patch test
 $E = 1.0$, $\nu = 0.25$, size $6 \times 3 \times 1$

Fig. 5.9 shows a patch of elements subjected to a load simulating the constant strain condition (Wilson and Ibrahimbegovic 1990). Elements need to satisfy the constant strain patch test only when the elements shrink to an infinitely small size. The tip displacements and average stresses obtained from these tests are shown in table 5.7

and table 5.8 respectively. Results are also compared with that of ANSYS. Here it has been found that with zero level of refinement, the solutions obtained from SFCSS are not exactly matching the theory. The percentage errors in the computed values of displacements and stresses are 18 and 14 respectively. After two levels of refinement (a refinement is obtained by joining the midpoints of an element in one plane to obtain four smaller elements), the displacements and stresses do converge to the exact solution. The percentage errors in the case of tip displacements and stresses reduced to 2.5 and 2 respectively.

Table 5.7 Tip displacements from constant strain patch test

Refinement level	ANSYS	SFCSS	THEORY
0 (5 elements)	6.0	7.08	6.0
2 (20 elements)	6.0	6.15	6.0

Table 5.8 Average stresses (σ_{xx}) from constant strain patch test

Refinement level	ANSYS	SFCSS	THEORY
0 (5 elements)	1.0	1.14	1.0
2 (20 elements)	1.0	1.02	1.0

5.5.2 Weak patch test

A unit extension load is applied on the beam, which is idealized with four undistorted elements as shown in the fig.5.10. Table 5.9 shows the stresses predicted within the patch at the various points calculated from the elements on either side of the respective points. It can be seen that the stresses computed are constant as required for

the patch test and the maximum deviation from the theoretical value is of the order of 2 percentage.

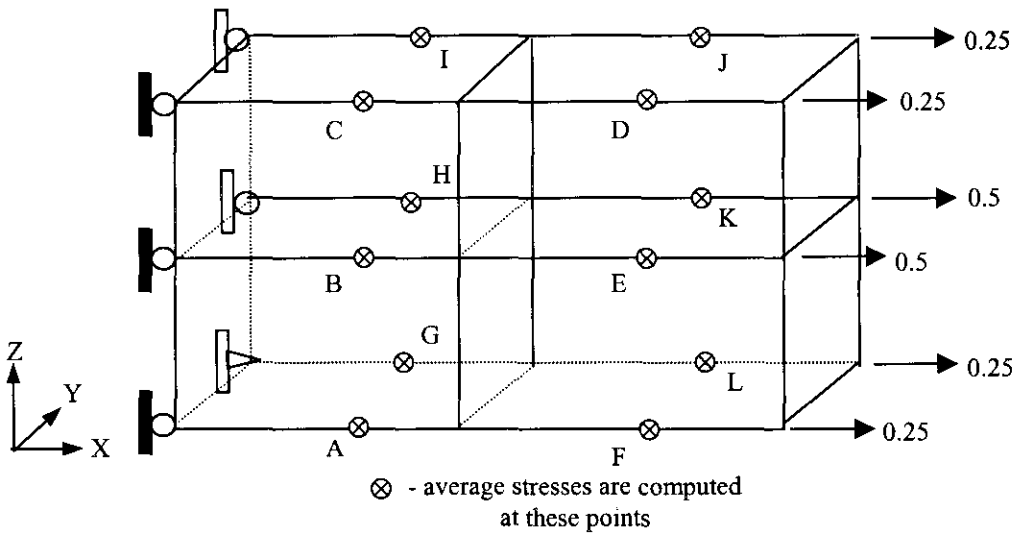


Fig. 5.10 Weak Patch test - Element geometry
 $E = 1.0, \nu = 0.1, \text{ size } 8 \times 2 \times 1$

Table 5.9 Stresses at different points from weak patch test

Location	STRESS σ_{xx}	
	SFCSS	THEORY
A	1.000	1.0
B	1.000	1.0
C	1.000	1.0
D	0.980	1.0
E	0.990	1.0
F	0.987	1.0
G	0.980	1.0
H	0.990	1.0
I	1.000	1.0
J	1.001	1.0
K	1.002	1.0
L	0.990	1.0

It is also observed that the stresses predicted at a point lying in a common boundary of elements are also found to be equal when it is computed from the stiffness matrices of each of the elements in which the elements are lying.

5.6 Boussinesq Problem

Boussinesq problem of an elastic half space with a point load approximated to a cylindrical volume is described in fig.5.11 (Bachrach 1987). The bottom surface ($z = -45$) is completely constrained. In order to represent symmetry about $x = y = 0$, XZ plane is constrained at $y = 0$ and YZ plane is constrained at $x = 0$. The material properties used are $E = 10^7$ units and $\nu = 0.3$. A concentrated load of 10,000 units is applied in the $-Z$ direction at the point A. Displacement at various points in $-Z$ direction are evaluated and compared with theoretical solutions (Bachrach 1987) in table 5.10. It has been found that the solutions obtained with SFCSS agree fairly well with the theory.

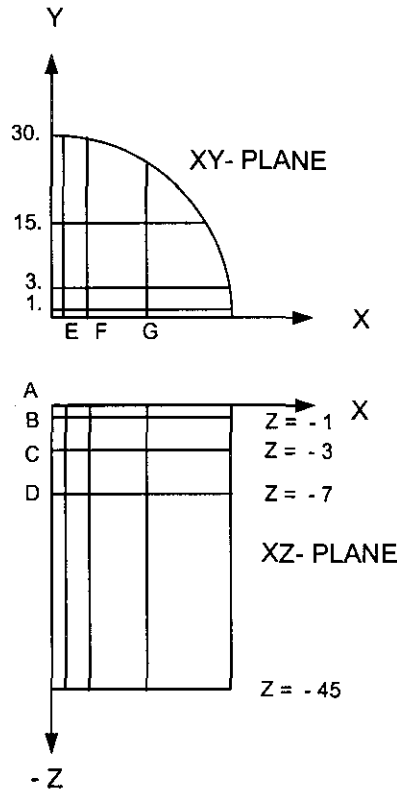


Fig. 5.11 Boussinesq problem for a cylindrical volume

Table 5.10 Results from the Boussinesq problem of cylindrical volume(- Z direction displacements $\times 10^{+5}$ at different points)

Element	A	B	C	D	E	F	G
H(8)*	-146.02	-43.08	-43.08	-4.70	-12.0	-7.46	-2.69
ANSYS	-162.72	-43.68	-9.39	-5.98	-12.79	-8.5	-3.49
SFCCS	-203.60	-44.70	-14.4	-6.20	-24.30	-9.8	-4.20
THEORY*	∞	-49.60	-16.6	-7.09	-29.00	-11.47	-4.83

*Source : Bachrach (1987)

5.7 Curved shell test

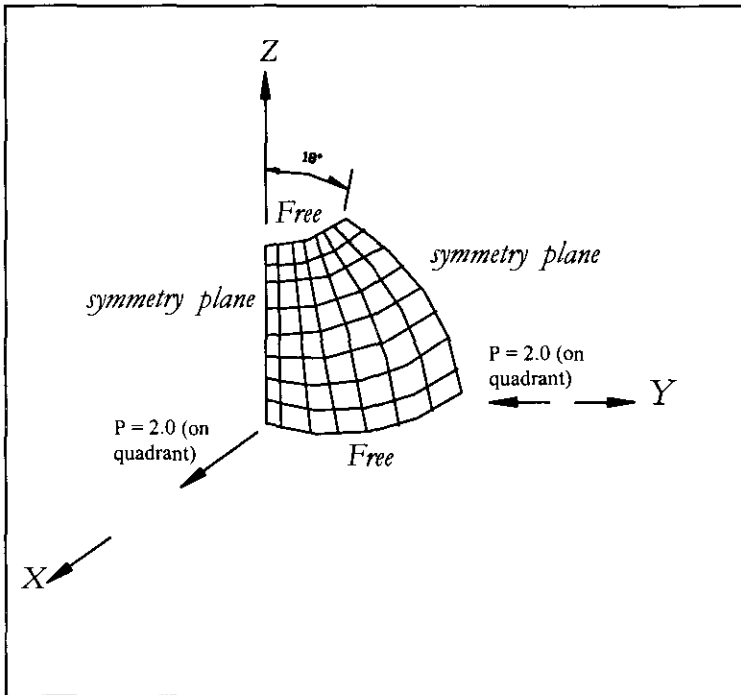
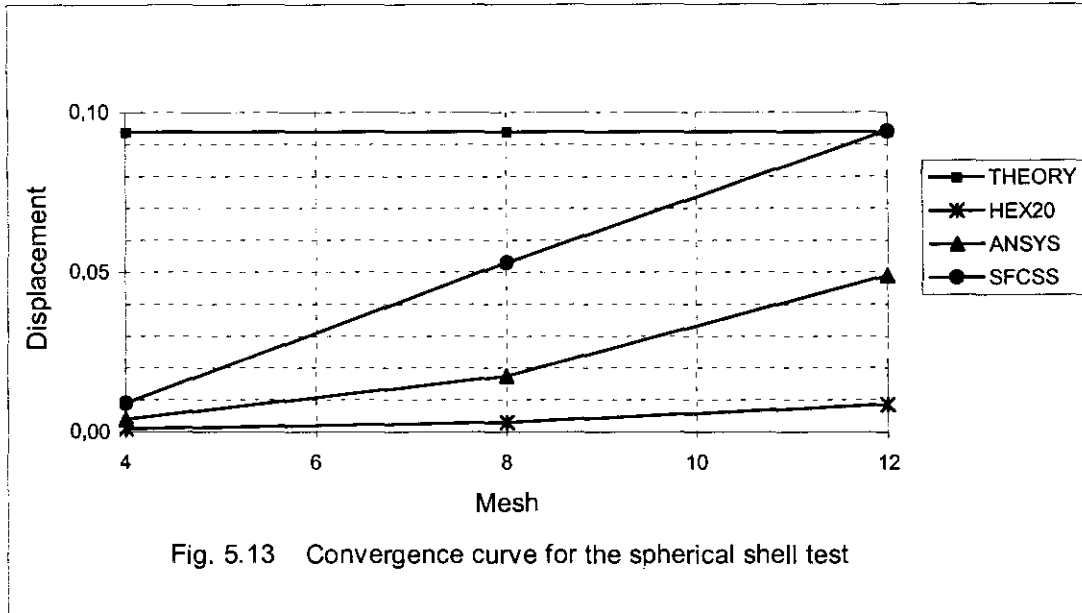


Fig. 5.12 Element mesh for curved shell test.
radius – 10, thickness – 0.04, E – 6.825×10^7 units, ν - 0.3

Doubly curved shell (spherical shell) problem proposed by MacNeal and Harder (1985) is dealt with. The hemispherical shell shown in fig. 5.12 is a doubly curved

shell, which is subjected to a *pinching* load. Two diametric compressive concentrated loads and two similar tension loads are applied on the shell. Both membrane and bending strains contribute significantly to the radial displacement at the point of application of the load (MacNeal and Harder 1985).



The results for the displacement at the point of application of the load obtained with SFCSS is compared with that from the existing elements and also with the theoretical solution (0.094) given by the MacNeal and Harder in fig.5.13. The exact value is recently modified by Simo and co-workers (1989) as 0.093. Here it can be seen that the solutions obtained from SFCSS converges quickly to the exact solution. They converge faster than those obtained from many other commercially available elements.

5.8 Remarks

The proposed element has been tested in standard test problems available in the literature. From these tests it is found that the new element performs very well in all the situations considered, except in patch test. SFCSS is a nonconforming element, as the displacements of points along the edges of the element are not fully depend on the nodes lying in that edge. Hence, it passes the patch test only in an average sense. However the element does pass the weak patch test and gives consistently good results in all the other test problems considered. In many cases convergence is faster when compared with other commonly available elements in the literature and those in commercially available programs like ANSYS.

CHAPTER 6

PERFORMANCE COMPARISONS OF PLATE BENDING ELEMENT (SFCFP)

6.1 Introduction

The development of a simple, four node quadrilateral plate bending element-SFCFP, in which the assumed displacement functions satisfy the differential equations of stress field equilibrium was described in chapter 3. SFCFP is a four node quadrilateral element with three degrees of freedom w , $\partial w/\partial x$ and $\partial w/\partial y$ at each node. The element geometry of SFCFP was shown in fig.3.3 The numerical investigation of the element performance has been carried out by testing it in standard test problems available finite element literatures and the results are compared with exact solutions and the results obtained with other established displacement based finite elements.

6.2 Eigenvalue test

The eigenvalue test is one of the important test for element quality. The test can detect zero energy deformation modes, lack of invariance and absence of rigid body motion capability. It can also be used to estimate the relative quality of different elements. An unrestrained element is considered for the eigenvalue test, so that $[k]$ is complete element stiffness matrix.

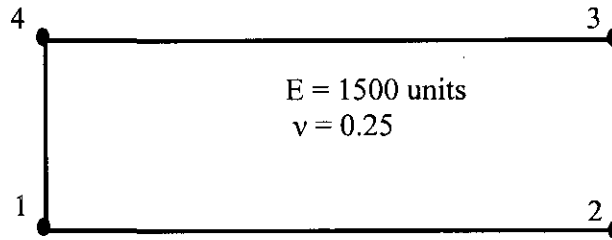


Fig 6.1 Eigenvalue test model using single element

A beam of size $10 \times 1 \times 1$ is modeled with a single element as shown in fig. 6.1. Material properties are considered as $E = 1500$ and $\nu = 0.25$. The element stiffness matrix and global stiffness matrix are same for this problem. The element has 3 dof per node and 12 dof in total. Stiffness matrix and eigenvalues of unrestricted element are calculated using the computer code plbe.for and are given in table 6.1. All the 12 eigenvalues are real and positive. Among them, three zeros or near zero values are obtained, showing that the element is exhibiting three rigid body modes.

Table 6.1 Eigenvalues computed from stiffness matrix of SFCSS

Sl No.	Eigenvalues	Sl No.	Eigenvalues	Sl No.	Eigenvalues
1	0.86804E+04	5	0.27911E+04	9	0.14213E+03
2	0.86804E+04	6	0.20888E+04	10	0.19256E-13
3	0.52617E+04	7	0.20888E+04	11	0.32422E-13
4	0.35714E+04	8	0.19231E+04	12	0.13224E-12

When the element is reoriented in global co-ordinates by changing the node numbering sequence, the eigenvalues do not change, indicating the geometric invariance of the

element. Hence, it is inferred that the stiffness matrix is real, positive semi definite and the element is geometrically isotropic.

6.3 Single element test

Most plate-bending element, including the present one, behave well in bending. The critical test for a single element is usually the twist moment with one edge fully camped, which activates differential (bilinear) bending (Robinson 1976). In this test, a one edge fully clamped cantilever plate of unit width is modelled with a single element as shown in fig.6.2

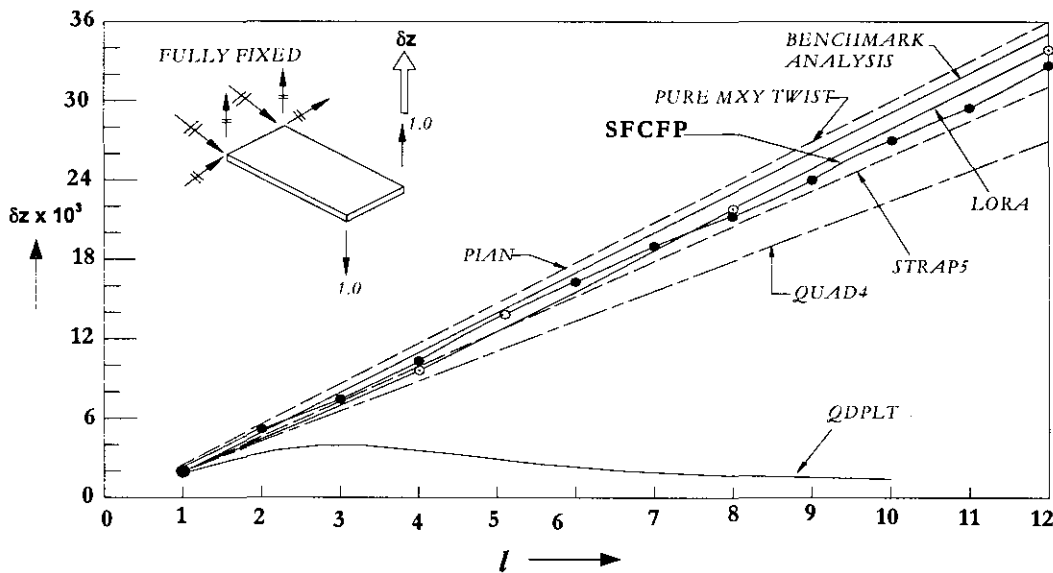


Fig. 6.2 Single element results, twist case using differential loads

A unit twisting moment is applied on the free edge of the plate. The plate thickness is taken as $t = 0.05$ units and material properties are $E = 10^7$ units and $\nu = 0.25$. The vertical displacements w of a free corner is plotted against element aspect ratio l in the

same figure. The results are also compared with the benchmark analysis results, which were obtained using sixteen high precision rectangles (STRAP5) (Hubka 1972). The figure also compares the results of LORA (Robinson and Haggemacher 1977), a four noded plate element based on stress assumptions, old NASTRAN plate bending element (QDPLT) (MacNeal 1969) and the new MSC/ NASTRAN element (QUAD4) (MacNeal 1976). The STRAP5, QDPLT and QUAD4 elements are all based on displacement assumptions. The plate-bending element PIAN (Pian 1965) is also based on stress assumptions with nine independent force variables. It is emphasized that there are three degrees of freedom per node for LORA, QDPLT, QUAD4 and PIAN, and four degrees of freedom per node for STRAP5. All elements have four nodes. Results obtained with SFCFP, LORA and STRAP5 are close to the benchmark analysis and almost unaffected by the variation in aspect ratio. Elements QUAD4 and QDPLT showed poor performance in this test.

6.4 Convergence test

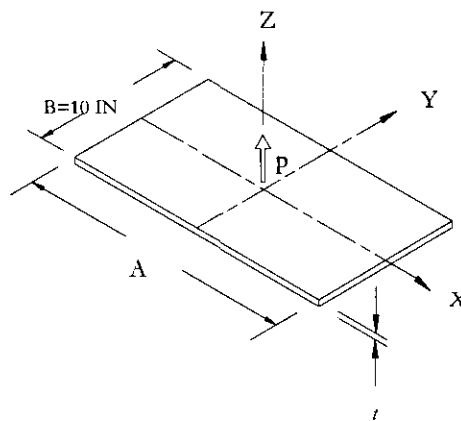


Fig. 6.3 Rectangular plate structure parameters for convergence test

$$E = 1000.0 \text{ LBS}, E = 30 \times 10^6 \text{ LB/IN}^2, \nu = 0.3, t = 0.1 \text{ IN}$$

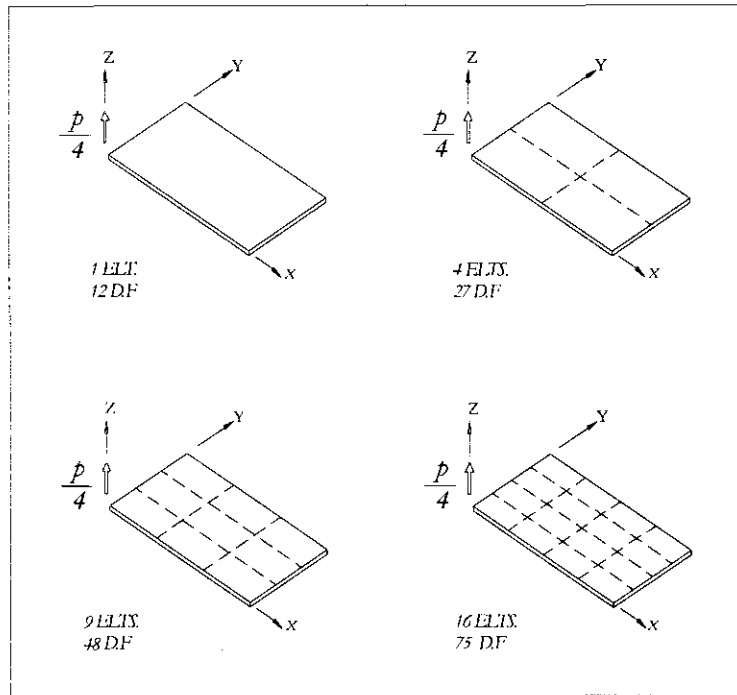


Fig. 6.4 Quarter plate finite element models

The convergence test (Clough and Tocher 1965, Robinson 1978) presented here, consists of investigating the central displacement of a rectangular plate with a centrally applied discrete load for two boundary conditions, simply supported and clamped. The plate problem is shown in fig. 6.3. To investigate the convergence characteristics of the plate element the variation of central displacement is studied using four different quarter plates meshes as shown in fig.6.4. For each mesh, the aspect ratio of the element and hence that of the plate is varied from 1 to 3.

The convergence results (central displacement w) obtained with SFCFP are compared with that of LORA, STRAP5, QDPLT, QUAD4 and PIAN elements in fig. 6.5 – 6.10. Theoretical solutions given by Timoshenko are also plotted in the respective figures for comparison purpose.

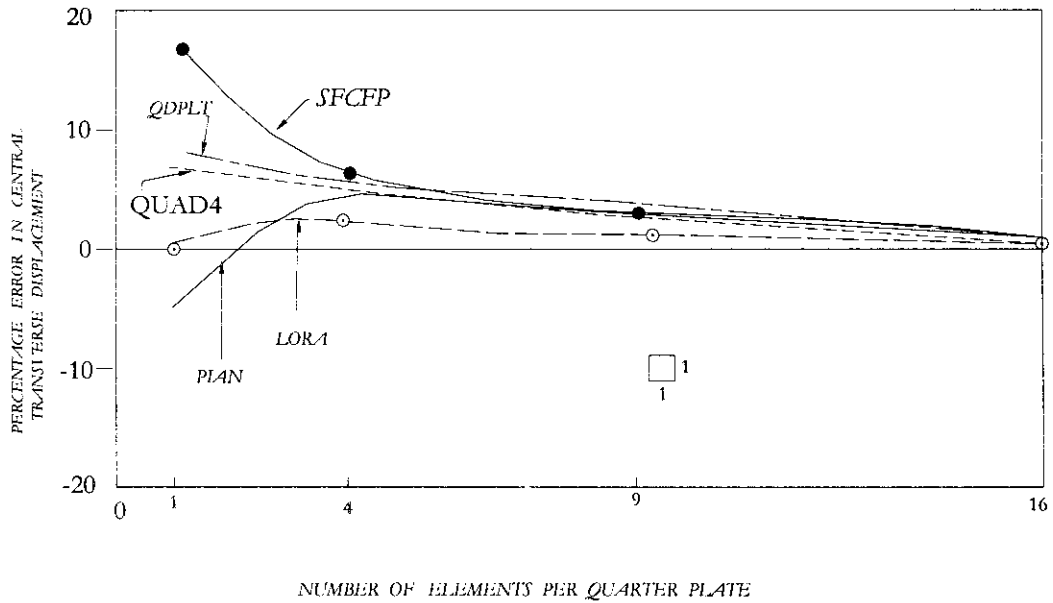


Fig. 6.5 Convergence results for a simply supported plate with a central point load and aspect ratio one

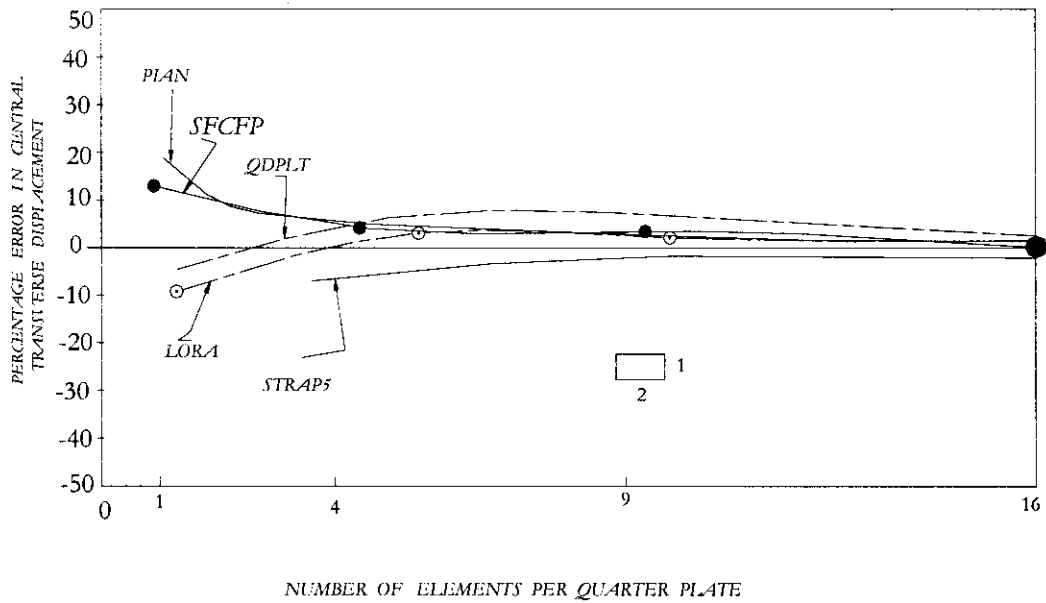


Fig. 6.6 Convergence results for a simply supported plate with a central point load and aspect ratio two

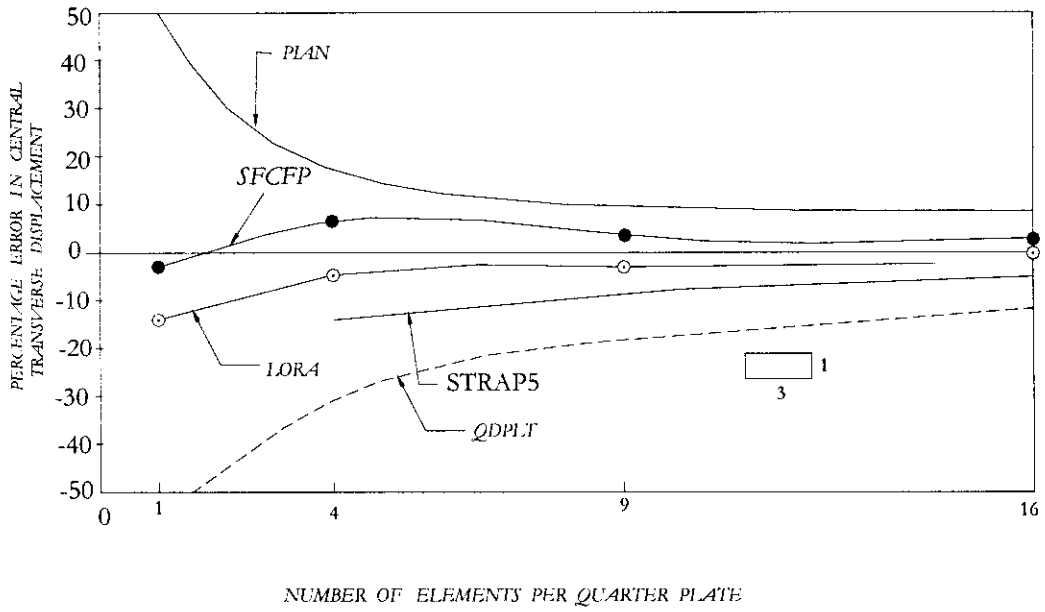


Fig. 6.7 Convergence results for a simply supported plate with a central point load and aspect ratio three

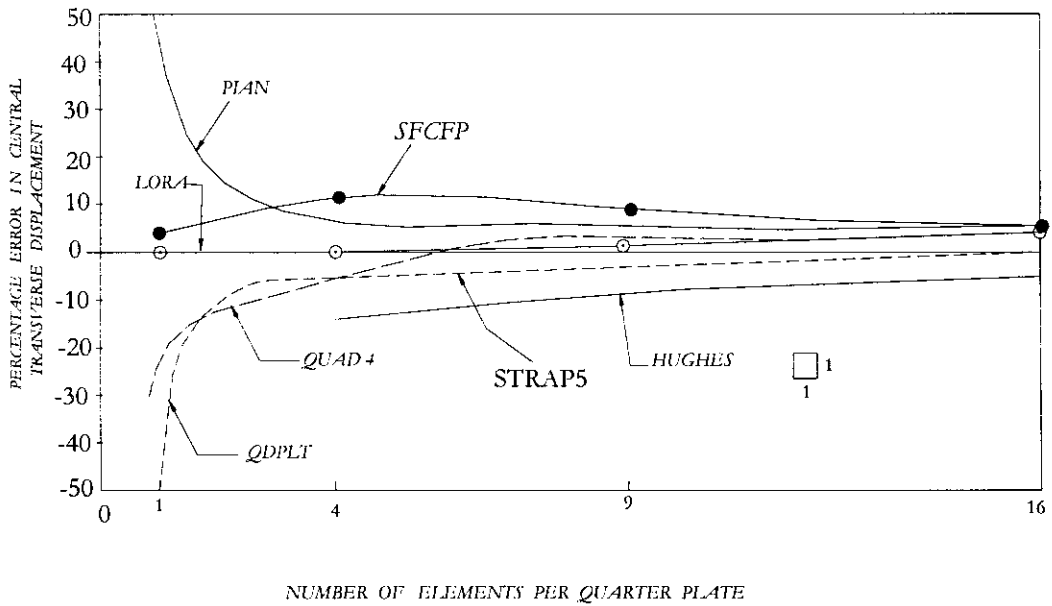


Fig. 6.8 Convergence results for a clamped plate with a central point load and aspect ratio one

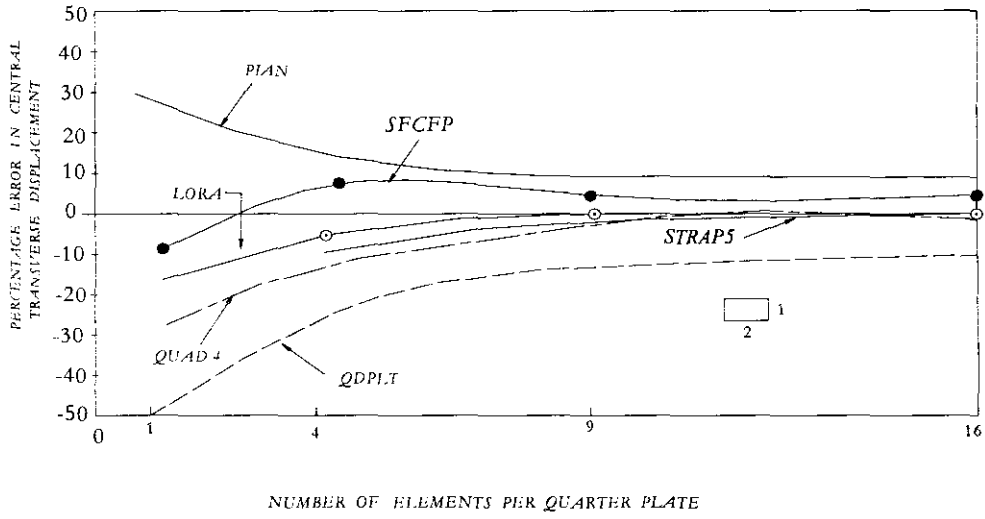


Fig. 6.9 Convergence results for a clamped plate with a central point load and aspect ratio two

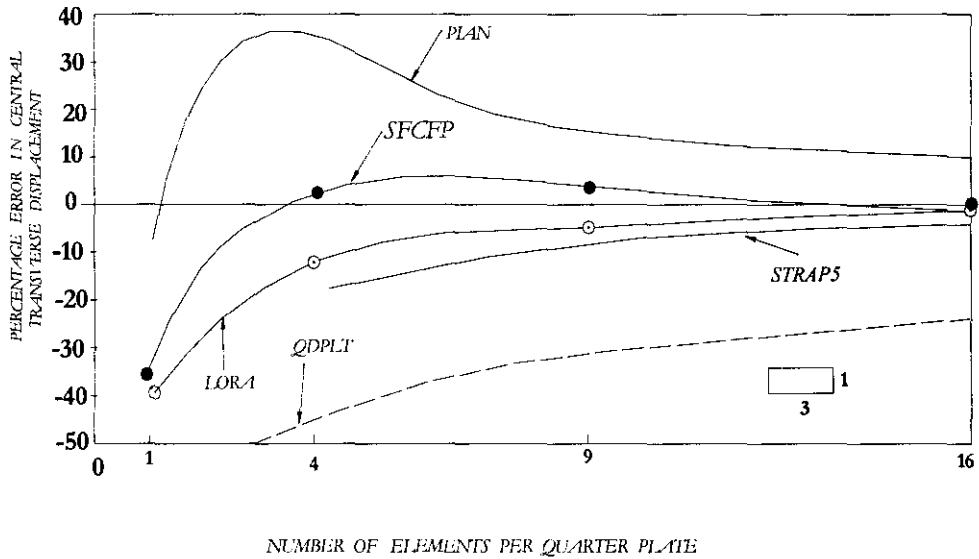


Fig. 6.10 Convergence results for a clamped plate with a central point load and aspect ratio three

It can be seen that almost all elements considered except QDPLT converged to exact solutions for all the three aspect ratios and boundary conditions. When the aspect ratio increases beyond 1, the accuracy of the solutions obtained from SFCFP improves and at higher aspect ratios, it out performed all the other elements including the elements like PIAN and LORA, which are used in commercially available finite element packages.

6.5 Remarks

The performance of the Plate bending element is evaluated using **a.** Single element test using cantilever with aspect ratios ranging from 1 to 12 under twist load. **b.** Convergence test using simply supported plate under central load with different aspect ratios. **c.** Convergence test using clamped plate under central load with different aspect ratios. The performance of element was found to be encouraging.

CHAPTER 7

CONCLUSION

7.1 Summary

This thesis deals with the formulation and development of plane stress, solid and plate bending finite elements for stress analysis, in which the displacement fields satisfy the differential equations of stress field equilibrium inside the element. A general procedure for the development of displacement functions which satisfy the corresponding stress field equilibrium equations has been detailed.

When differential equations of stress field equilibrium are imposed on the assumed displacement interpolation functions, several linear constraints on the set of unknown coefficients of the polynomial emerge. These constraints reduce the total number of unknown coefficients and hence a higher order polynomial can be used to interpolate the displacements inside the element. This makes the element nonconforming. Some of the existing nonconforming elements are made compatible with various schemes. However the stress field equilibrium is attained only when the mesh is made extremely fine. In the proposed elements, *a priori* satisfying the stress field equilibrium would make the element attractive, despite the incompatibility there by induced.

By incorporating displacement fields that satisfy the stress field equilibrium inside the element based on displacement approach, the finite element model will not only have the equilibrium between the applied loads and elemental forces (in an integral sense) at the nodes, but also have the stress fields in each element in equilibrium. The displacement interpolation functions inside each individual element are truncated

polynomial solutions of differential equations. In fact the finite element solution will now represent a patch wise approximation of the state of stress inside the element.

The approach to develop the field equilibrium elements is quite general and various elements to analyse different types of structures can be formulated from the corresponding stress field equilibrium equations. Using this procedure, a nine node quadrilateral plane stress element (SFCNQ), a sixteen node brick element (SFCSS) for three dimensional stress analysis and a four node plate bending element (SFCFP) have been formulated. For implementing these elements, computer programs based on modular concepts have been developed.

The performance of these elements have been investigated with standard test problems reported in the literature and the results are compared with the theoretical closed form solutions and that obtained with other existing elements. It is found that the new elements perform well in all the situations considered. However, due to its nonconformity, the elements pass the patch test with distorted geometry, only in an average sense. But they do pass the patch test with undistorted element geometry (weak patch test) and solutions in all the cases converge correctly to the exact values. In many cases convergence is faster when compared with other commonly available elements in finite element literature and those in commercially available programs like ANSYS. The behaviour of field consistent elements would definitely generate a great deal of interest amongst the users of the finite elements.

7.2 Scope for future work

The elements demonstrated consistently good performance over other elements in the test problems considered and solutions in all the cases converge correctly to the exact

values. The family of field equilibrium elements is worthy of consideration by analysts. However, a more thorough investigation is required to establish the concept proposed in this thesis. To exploit the potential of these elements completely the following issues have to be addressed.

As these elements are nonconforming, and the extent of nonconformity increases with the order of the element, the efficiency of each individual element with respect to the appropriate test problems needs to be investigated. A formal error analysis for these elements needs to be undertaken. The reliability of these elements should be established with more stringent convergence tests. Computational cost efficiency comparison studies with other existing elements have to be conducted. There is sufficient scope for development of field equilibrium finite elements to deal with structural problems involving orthotropic and anisotropic materials.

REFERENCES

1. Ahmad S. and B.M. Irons (1974) An assumed stress approach to refined isoparametric finite elements in three dimensions. In *Finite element methods in engineering*, University of New South Wales.
2. Argyris J.H. and I. Fried (1968) The LUMINA element for the matrix displacement method. *The Aeronautical Journal of the Royal Aeronautical Society*, **72**:514-517.
3. Bachrach W.E. (1987) An efficient formulation of hexahedral elements with high accuracy for bending and incompressibility. *Journal of Computers and Structures*, **26**:450 - 467.
4. Bathe K.J., J.L. Batoz and L.W. Ho (1980) A study of three node triangular plate bending elements. *International Journal for Numerical Methods in Engineering* **15**:1771-1812.
5. Bathe K.J. *Finite element procedures in engineering analysis*, Prentice Hall Inc. Englewood cliffs, New Jersey, 1982.
6. Bathe K.J. and E.N. Dvorkin (1985) A four node plate bending element based on the Mindilin/Reissner plate theory and mixed interpolation. *International Journal for Numerical Methods in Engineering*, **21**:367-383.
7. Bogner F.K., R.L Fox and L.A. Schmidt (1965) The generation of inter element Compatible stiffness and mass matrices by the interpolation Formulae. *Proc. of the conference on matrix methods in structural mechanics*, Wright Patterson Air Force Base, Ohio.
8. Chandra. S. and G. Prathap (1989) A field consistent formulation for the eight noded solid finite element. *Comput. and Struct.*, **33**:345 –355.
9. Chen W. and Y.K. Cheung (1987) A new approach for hybrid element method. *International Journal for Numerical Methods in Engineering*, **24**:1697-1709.
10. Chen W. and Y.K. Cheung (1992) Three Dimensional 8- node and 20 node refined hybrid isoparametric elements, *International Journal for Numerical Methods in Engineering*, **35**:1871 –1889.
11. Cheung Y.K. and Wanji Chen (1988) Isoparmetric hybrid hexahedral elements for three dimensional stress analysis. *International Journal for Numerical Methods in Engineering*, **26**:677-693.

12. Clough R.W. (1960) The finite element method in plane stress analysis. *Proceedings of American Society of Civil Engineers*, 2nd conference on Electronic Computations, Pittsburgh, Pennsylvania, **23**:345-378.
13. Clough R.W. and J.L Tocher (1965) Finite element stiffness matrices for analysis of plate bending. *Proc. First. Conf. Matrix. Methods. in Struct. Mechanics*, Wright-Patterson A.F.B., Ohio, USA, AFFDL-TR-66-88.
14. Clough R.W. and C.A. Felippa (1968) A refined quadrilateral element for the analysis of plate bending. *Proc. of the Conference on Matrix Methods in Structural Mechanics*, Wright Patterson Air force base, Ohio.
15. Clough R.W. (1969) Comparison of three dimensional finite elements. In W H Rowan and R M Hackett, editors, *Symposium on application of finite element methods in civil engineering ASCE*, Vanderbilt university, Nashville, Tenn.
16. Collatz L. *The Numerical Treatment of Differential Equations*, Springer - Verlag, Berlin, 1950.
17. Conte S.D. and C. de Boor, *An introduction to numerical analysis-An algorithmic Approach*, McGraw Hill Singapore, 1980.
18. Cook R.D. and Jaafar K. Al Abdulla (1969) Some plane quadrilateral hybrid finite elements. *AIAA Journal*, **11**:2184-2185.
19. Cook R.D. (1969) Strain resultants in certain finite elements. *American Institute of Aeronautics Journal*, **7**:535.
20. Cook R.D. (1977) More about artificial softening of finite elements. *International Journal for Numerical Methods in Engineering*, **11**:1334-1339.
21. Cook R.D., S. Malkus and E. Plesha, *Concepts and Applications of Finite Element Analysis*, John Wiley and Sons, 1989.
22. Courant R. (1943) Variational methods for the solution of problems of equilibrium and vibrations. *Bulletin of the American Mathematical Society*, **49**:1 –23.
23. Courant R. and D. Hilbert, *Methods of Mathematical Physics*, John Wiley and Sons, New York, 1953.
24. Desai C.S. and J.F. Abel, *Introduction to the finite element method*, Van Nostrand Reinhold Co., New York, 1972.
25. Dow J.O., T.H. Ho and H.D. Cabiness (1984) Generalized Finite Element Evaluation Procedure. *Journal Of Structural Engineering*, **3**: 435 – 452.
26. Dvorkin E.N. and K.J. Bathe, *Engineering Computations*, Pineridge Press, 1984.

27. Fried I. (1975) Finite element Analysis of thin elastic shells with residual energy balancing and the roll of rigid body modes. *International journal for Applied Mechanics*, **42**:99-104.
28. Gallagher R.H., J. Padlog and P.P. Bijlard (1962) Stress analysis of heated complex shapes. *Journal of American Rocket Society*, **32**:700-707.
29. Heppler G.R. and J.S. Hanson (1987) Timoshenko beam finite elements using trigonometric basis functions. *AIAA Journal*, **26**:1378-1386.
30. Hubka R.E. (1972) Buckling Analysis of Stiffened curved and flat rectangular plates. *Lockheed-California Company Report Number LR 25381*.
31. Hughes T.J.R. and H. Allik (1969) Finite elements for compressible and incompressible continua. In W H. Rowan and R M. Hackett, editors, *Symposium on application of finite element methods in civil engineering*, ASCE, Vanderbilt University, Nashville, Tenn.
32. Hughes T.J.R., R.L. Taylor and W. Kanoknukulchai (1977) A simple and efficient finite element for plate bending. *International Journal for Numerical Methods in Engineering*, **11**:1529-1543.
33. Irons B.M., G.P. Bazeley, Y.K. Cheung and O.C. Zeinkiewicz (1965) Triangular Elements in Plate Bending – Conforming and Nonconforming Solutions. *Proc. First Conf. on Matrix Methods in Structural Mechanics*, Wright – Patterson Air Force Base, Ohio, 547 –567.
34. Irons B.M. (1972) An assumed stress version of the Wilson Eight node brick. *University of Wales, Computer report CNME/CR/56*.
35. MacNeal R.H. (1969) NASTRAN Theoretical Manual, *NASA Report under contract Number NAS 5-10049*, Section 5.8.3.1.
36. MacNeal R.H. (1976) A simple quadrilateral shell element. *MacNeal - Schwendler Report Number 52*.
37. MacNeal R.H. (1982) Derivation of assumed stress matrices by assumed strain distributions. *International Journal for Nuclear Engineering Design*, **70**:3-12.
38. MacNeal R.H. and R.L. Harder (1985) A proposed set of problems to test the finite element accuracy. *Finite element in analysis and design* **1**:3-20.
39. MacNeal R.H. (1987) A theorem regarding the locking of tapered four noded membrane elements. *International Journal for Numerical Methods in Engineering*, **24**:1793-1799.

40. MacNeal R.H. (1992) On the limits of finite element perfectibility. *International Journal for Numerical Methods in Engineering*, **35**:1589-1601.
41. Melosh R.J. (1963 a.) Structural analysis of solids. *Journal of the Structural Division, ASCE*, **89**:205-223.
42. Melosh R.J. (1963 b.) Basis of derivation of matrices by the direct stiffness method. *AIAA Journal*, **1**:1631-1637.
43. Melosh R.J. (1963 c.) Rectangular plate element with 12 dof.- Basis for derivation of matrices by the direct stiffness method. *AIAA Journal*, **1**: pp 1631-1637.
44. Park K.C. (1984) Symbolic Fourier analysis procedures for C^0 finite elements. *Innovative methods for Non linear analysis*, **11**:269-293.
45. Pian T.H.H. (1965) Element stiffness matrices for boundary compatibility and for prescribed boundary stresses. *Proc. First. Conf. Matrix. Methods. in Struct. Mechanics*, Wright-Patterson A.F.B., Ohio, USA, AFFDL-TR-66-88.
46. Pian T.H.H. (1973) Hybrid model. In S J Fenves, N Perrone, A.R.Robinson and W C Schnobrich, editors, *Numerical Methods and Computer Methods in Applied Mechanics*, Academic Press , New York.
47. Prathap G. (1985) A C^0 continuous four noded cylindrical shell element. *International Journal for Comp. and Structures*, **21**:995-999.
48. Prathap G. (1986) Field consistency – toward a science of constrained multi strain field finite element formulation. *Sadhana- Proc. Eng. Sci. Ind. Acad. of Sci.*, **9**:319-344.
49. Prathap G. (1992) Recent advances in finite element technology. *NAL-UNI Series*, NAL, Bangalore.
50. Rashid Y.R., P.D. Smith and N. Prince (1969) On further application of finite element method to three dimensional elastic analysis, In W H Rowan and R M Hackett, editors, *Symposium on high speed computing of elastic structures*, ASCE, Vanderbilt University, Nashville, Tenn.
51. Rashid Y.R., P.D. Smith and N. Prince (1969) Three dimensional analysis of elastic solids I Analysis Procedure. *International Journal of Solids and Structures*, **5**: 1311-133.
52. Rashid Y.R., P.D. Smith and N. Prince (1970) Three dimensional analysis of elastic solids II. The computational problems. *International Journal of Solids and Structures*, **6**:195-207.

53. Robinson J. (1976) A Single Element Test. *International Journal for Computer Meth. Appl. Mech. Engng*, **7**:191-200.
54. Robinson J. and G.H. Haggemacher (1977) LORA - An accurate four node plate bending element. *Lockheed California company report number LR 28386*.
55. Robinson J. (1978) Element evaluation – a set of assessment points and standard tests. *Proc. Second World Congress in Finite Element Methods*, Robinson and Associates, Dorset, England.
56. Robinson J. (1986) New FEM user project: Single element test for aspect ratio sensitivity – Part I. *Finite Element News*, Issue 1, February, 26-32.
57. Saleeb A.F. and T.Y. Chang (1987) Hybrid / Mixed Formulations. *International Journal for Numerical Methods in Engineering*, **24**:1123-1155.
58. Simo C., D.D. Fox and M.S. Rifai (1989) On a stress resultant geometrically exact shell model Part II: The linear theory and computational aspects. *Comp. Methods in Appl. Mech. Engg*, **73**: 53-92.
59. Spilker R.L. (1981) High order three dimensional hybrid stress elements for thick plate analysis. *International Journal for Numerical Methods in Engineering*, **17**:53-69.
60. Strang G. and G. Fix, *An Analysis of Finite Element Method*, Prentice-Hall, Englewood Cliffs, New Jersey, 1972.
61. Synge J.L., *The Hypercircle in Mathematical Physics*, Cambridge University press, London, 1957.
62. Sze K.Y. and A. Ghali (1993) Hybrid hexahedral elements for solids, plates, shells and beams by selective scaling. *International Journal for Numerical Methods in Engineering*, **36**:1519-1540.
63. Tang L. and W. Chen (1982) The non-conforming finite element for stress analysis In G. He and Y K. Cheung, editors *Proceedings in the International Conference on Finite Element Methods*, Gordon and Breach, New York.
64. Taylor R.L., P.J. Beresford and E.L. Wilson (1976) A nonconforming element for stress analysis. *International Journal for Numerical Methods in Engineering*, **10**:1211-1219.
65. Tessler A. and S.B. Dong (1981) On a hierarchy of conforming beam elements. *International journal for Computers and Structures*, **14**:335-344.
66. Timoshenko S.P. and J.N. Goodier, *Theory of Elasticity*, McGraw Hill, New–York, 1972.
67. Turner M.J., R.W. Clough, H.C. Martin and L.J. Topp (1956) Stiffness and deflection analysis of complex structures. *International Journal of Aeronautical Science*, **23**:805-823.

68. White D.W. and J.F. Abel (1989) Testing of shell finite element accuracy and robustness. *Finite element in Analysis and Design*, **6**:129-151.
69. Wilson E.L. (1973) Incompatible displacement models. In S J. Fenves, N. Perrone, A. R. Robinson and W C. Schnobrich, editors, *Numerical Methods and Computer methods in Applied Mechanics*, Academic Press, New York.
70. Wilson E.L., R.L. Taylor, W.P. Doherty and J. Ghaboussi (1973) Incompatible displacement models. In S.J. Fenves, N. Perrone, A.R. Robinson and WC. Schnobrich, editors, *Numerical and Computer Methods in Structural Analysis*, Academic press, New York.
71. Wilson E.L. and A. Ibrahimbegovic (1990) Use of incompatible displacement modes for the calculation of element stiffnesss or stresses, *Finite Elements in Analysis and Design*, **7**: 229-241.
72. Yang T.Y., *Finite Element Structural Analysis*, Prentice Hall, Engle wood Cliffs, New Jersey, 1986.
73. Zienkiewicz O.C., R.L. Taylor and J.M. Too (1971) Reduced integration technique in general analysis of plates and shells. *International Journal for Numerical Methods in Engineering*, **3**:275-290.
74. Zienkiewicz O.C. and R.L. Taylor, *The Finite Element Method Vol. I Basic Formulation and Linear problems*, McGraw Hill, New York, 1989.
75. Zienkiewicz O.C. and R.L. Taylor, *The finite element method Vol 2, Solid and Fluid Mechanics, Dynamics, Nonlinearity*, McGraw Hill Book Co. UK, 1991.

APPENDIX 1

CONSTRAINT EQUATIONS ON UNKNOWN COEFFICIENTS FOR THE DEVELOPMENT OF PLANE STRESS ELEMENT – SFCNQ (REF 3.2.1)

$$2a_5 + vb_4 + r(2a_6 + b_4) = 0 \quad (A1.1)$$

$$2b_6 + va_4 + r(2b_5 + a_4) = 0 \quad (A1.2)$$

$$3a_9 + vb_7 + r(a_8 + b_7) = 0 \quad (A1.3)$$

$$b_8 + va_7 + r(3b_9 + a_7) = 0 \quad (A1.4)$$

$$a_7 + vb_8 + r(3a_{10} + b_8) = 0 \quad (A1.5)$$

$$3b_{10} + va_8 + r(a_8 + b_7) = 0 \quad (A1.6)$$

$$3a_{12} + 2vb_{11} + r(3a_{13} + 2b_{11}) = 0 \quad (A1.7)$$

$$3b_{13} + 2va_{11} + r(3b_{12} + 2a_{11}) = 0 \quad (A1.8)$$

$$12a_{14} + 3vb_{12} + r(2a_{11} + 3b_{12}) = 0 \quad (A1.9)$$

$$2b_{11} + 3vb_{13} + r(12b_{14} + 3a_{12}) = 0 \quad (A1.10)$$

$$2a_{11} + 3vb_{13} + r(12a_{15} + 3b_{13}) = 0 \quad (A1.11)$$

$$12b_{15} + 3va_{13} + r(2b_{11} + 3a_{13}) = 0 \quad (A1.12)$$

Where ν is the poisson's ratio and $r = (1-\nu)/2$

Constraint equations A1.1 and A1.2 are obtained by equating the constant coefficients of the two stress field equilibrium equations equal to zero. Equations A1.3 and A1.4 are obtained by equating the coefficients of x equal to zero. Equations A1.5 and A1.6 are obtained by equating the coefficients of y equal to zero. Equations A1.7 and A1.8 are obtained by equating the coefficients of x^2 equal to zero. Equations A1.9 and A1.10 are obtained by equating the coefficients of y^2 equal to zero. Equations A1.11 and A1.12 are obtained by equating the coefficients of xy equal to zero.

APPENDIX 2

CONSTRAINT EQUATIONS ON UNKNOWN COEFFICIENTS FOR THE DEVELOPMENT OF THREE DIMENSIONAL ELEMENT - SFCSS (REF 3.3.1)

$$2p_1a_5 + p_2b_6 + p_2c_7 + 2p_3a_8 + p_3b_6 + p_3c_7 + 2p_3a_{10} = 0 \quad (\text{A2.1})$$

$$2p_1b_8 + p_2a_6 + p_2c_9 + 2p_3b_{10} + p_3c_9 + p_3a_6 + 2p_3b_5 = 0 \quad (\text{A2.2})$$

$$2p_1c_{10} + p_2b_9 + p_2a_7 + 2p_3c_5 + p_3a_7 + p_3b_9 + 2p_3c_8 = 0 \quad (\text{A2.3})$$

$$6p_1a_{11} + 2p_2b_{12} + 2p_2c_{13} + 2p_3a_{16} + 2p_3b_{12} + 2p_3c_1 + 2p_3a_{19} = 0 \quad (\text{A2.4})$$

$$2p_1b_{16} + 2p_2a_{12} + p_2c_{14} + 2p_3b_{19} + p_3c_{14} + 2p_3a_{12} + 6p_3b_{11} = 0 \quad (\text{A2.5})$$

$$2p_1c_{19} + p_2b_{14} + 2p_2a_{13} + 6p_3c_{11} + 2p_3a_{13} + p_3b_{14} + 2p_3c_{16} = 0 \quad (\text{A2.6})$$

$$2p_1a_{12} + 2p_2b_{16} + p_2c_{14} + 6p_3a_{15} + 2p_3b_{16} + p_3c_{14} + 2p_3a_{20} = 0 \quad (\text{A2.7})$$

$$6p_1b_{15} + 2p_2a_{16} + 2p_2c_{17} + 2p_3b_{20} + 2p_3c_{17} + 2p_3a_{16} + 2p_3b_{12} = 0 \quad (\text{A2.8})$$

$$2p_1c_{20} + 2p_2c_{17} + p_2a_{14} + 2p_3c_{12} + p_3a_{14} + 2p_3b_{17} + 6p_3c_{15} = 0 \quad (\text{A2.9})$$

$$2p_1a_{13} + p_2b_{14} + 2p_2c_{19} + 2p_3a_{17} + p_3b_{14} + 2p_3c_{19} + 6p_3a_{18} = 0 \quad (\text{A2.10})$$

$$2p_1b_{17} + p_2a_{14} + 2p_2c_{20} + 6p_3b_{18} + 2p_3c_{20} + p_3a_{14} + 2p_3b_{13} = 0 \quad (\text{A2.11})$$

$$6p_1c_{18} + 2p_2b_{20} + 2p_2a_{19} + 2p_3c_{13} + 2p_3a_{19} + 2p_3b_{20} + 2p_3c_{17} = 0 \quad (\text{A2.12})$$

Where $p_1 = \frac{E\nu}{(1+\nu)(1-2\nu)} + \frac{E}{(1+\nu)}$, $p_2 = \frac{E\nu}{(1+\nu)(1-2\nu)}$ and $p_3 = \frac{E}{(1+\nu)}$.

Constraint equations A2.1, A2.2 and A2.3 are obtained by equating the constant coefficients of the three stress field equilibrium equations equal to zero. Equations A2.4, A2.5 and A 2.6 are obtained by equating the coefficients of x equal to zero. Equations A2.7, A2.8 and A2.9 are obtained by equating the coefficients of y equal to zero. Equations A2.10, A2.11 and A2.12 are obtained by equating the coefficients of z equal to zero.

PUBLICATIONS BASED ON THE RESEARCH WORK

1. Jayakumar. S and C.G. Nandakumar (2000) SFCFP - A stress field consistent four node plate bending element, *Proc. of the International Conference on Ship and Marine technology*, Cochin
2. Jayakumar. S and C.G. Nandakumar (2003) Field Equilibrium Finite Elements – A new family of elements for efficient and accurate finite element analysis *Proc. of the National Conference on Advances in Manufacturing Technology (AMT 2003)*, Palghat
3. Jayakumar. S and C.G. Nandakumar, SFCSS - A stress field consistent sixteen node solid element for three dimensional stress analysis. Communicated to *Journal of Computational Mathematics*, Chinese Academy of Sciences, Beijing, China.

G18546

